To the Graduate Council:

I am submitting herewith a thesis written by Clement C. Morlock Jr. entitled "Harmonic Losses Of A Three Phase Induction Motor When Powered From An Adjustable Frequency Inverter." I recommend that it be accepted in partial fulfillment of the requirements for the degree of Master of Science, with a major in Electrical Engineering.

Frederick W. Symonds

Dr. F. W. Symonds, Major Professor

We have read this thesis
and recommend its acceptance:

Thomas W. Worlock

Lincoln H. Turner

Accepted for the Council:

L. Evans Peck

Vice Chancellor
Graduate Studies and Research

Cop. 2

HARMONIC LOSSES OF A THREE PHASE INDUCTION MOTOR WHEN POWERED FROM AN ADJUSTABLE FREQUENCY INVERTER

A Thesis

Presented for the

Master of Science

Degree

The University of Tennessee, Knoxville

Clement C. Morlock Jr.

June 1977

1324115

ABSTRACT

New advances in solid state technology have resulted in solid state switches capable of handling considerable power. Inevitably, these devices have found applications as motor controllers. Resulting systems can control direction, speed, acceleration and slip. These capabilities enhance the already great advantages of the three phase induction motor. The area of investigation of this thesis is the effect these control systems can have on the performance of an induction motor.

Evolution and design trade-offs of these solid state circuits are considered. The equivalent motor circuit is developed using standard techniques. A dynamic inverter is used to operate the motor at non-standard speeds. Experimental and calculated performance data are carefully compared to check the validity of the analysis.

A static inverter is then used to power the motor. The line-to-neutral output voltage is a square wave. Using Fourier Analysis, the square wave is resolved into its fundamental components, and each component is then applied to the equivalent circuit. The calculated performance is a summation of these harmonic contributions. A comparison is made between experimental and calculated performance data. Projections of possible improvements in efficiency are made using idealized pulse waveforms.

Control systems utilizing an adjustable speed electric motor have great potential. They are currently being used in pumping applications, surface mining, chemical batch processing, and the textile industry. A huge potential market is the transportation industry. When suitable energy storage components become a reality, an electric vehicle will be able to use an adjustable speed electronic system. Applications to such a large market will result in a drastic reduction in cost and thus opening up many economically justifiable uses.

PREFACE

The drastic improvements in semiconductor components have resulted in a proliferation of variable speed motor controllers. These systems power motors with energy contained in a nonsinusoidal voltage envelope. This paper is a comparison of motor performance under harmonic rich variable frequency supply conditions and standard operating conditions. To provide test data, a three phase induction motor was operated from a sinusoidal source at three frequencies and a nonsinusoidal source at three frequencies. Complete load profiles were recorded for these six different conditions. Photographs of both line voltage and current were taken.

The steps involved in predicting motor performance for a nonsinusoidal voltage source are:

1. Determine harmonic content of voltage applied to the motor.
2. Use standard analysis techniques to obtain the equivalent circuit of the motor. The frequency dependent parameters of this circuit are scaled for calculations involving harmonic frequencies.
3. Apply superposition as appropriate to obtain composite motor response to a nonsinusoidal voltage waveshape.

The results of these calculations were compared to the

experimental data recorded. Potential efficiency improvements through harmonic power reductions are explored.

TABLE OF CONTENTS

CHAPTER		PAGE
I.	ADJUSTABLE SPEED ELECTRIC MOTOR SYSTEMS.	1
	Basic Motor Parameters	1
	Dynamic Adjustable Frequency Systems	3
	Static Adjustable Frequency Systems.	5
	Wave-converter	5
	Rectifier-inverter	7
II.	THE RECTIFIER-INVERTER SYSTEM.	14
	Three Phase Controlled Rectifier	14
	Transistor Inverter.	16
	Silicon Controlled Rectifier-Inverter.	18
	Three Phase Digital Logic.	21
III.	MOTOR PERFORMANCE CALCULATIONS--SINUSOIDAL VOLTAGE SOURCE	26
	Experimental Procedures.	26
	Rotational Losses.	27
	Equivalent Circuit Calculations.	28
	Performance Calculations Under Loaded Conditions	40
IV.	MOTOR PERFORMANCE--NONSINUSOIDAL SOURCE.	52
	Fourier Analysis	52
	Performance Calculations	55
	Waveform Analysis.	70
V.	SYSTEM PERFORMANCE CONSIDERATIONS.	81

CHAPTER PAGE

Motor Performance 81
Experimental and calculated data. 81
Efficiency improvements due to reduction in harmonic content. 82
Inverter Performance. 87
VI. CONCLUSIONS 89
BIBLIOGRAPHY. 91
APPENDIXES. 93
APPENDIX A. COMPUTER PROGRAMS. 94
APPENDIX B. TEST EQUIPMENT 99
VITA. 104

LIST OF TABLES

TABLE		PAGE
I.	Rotational Loss Data.	29
II.	No-Load Test Data	31
III.	Locked Rotor Test Data.	32
IV.	Performance Calculations (51 hz, 186 volts) . . .	41
V.	Performance Calculations (60 hz, 220 volts) . . .	42
VI.	Performance Calculations (75 hz, 272 volts) . . .	43
VII.	Experimental Performance Data (51 hz, 186 volts).	46
VIII.	Experimental Performance Data (60 hz, 220 volts).	47
IX.	Experimental Performance Data (75 hz, 272 volts).	48
X.	Results of Performance Calculations (20 hz, 115 volts P-P).	58
XI.	Results of Performance Calculations (40 hz, 210 volts P-P).	59
XII.	Results of Performance Calculations (60 hz, 270 volts P-P).	60
XIII.	Nonsinusoidal Measured Performance Data (20 hz, 115 volts P-P).	61
XIV.	Nonsinusoidal Measured Performance Data (40 hz, 210 volts P-P).	62
XV.	Nonsinusoidal Measured Performance Data (60 hz, 270 volts P-P).	63
XVI.	Inverter Performance Data	88

LIST OF FIGURES

FIGURE		PAGE
1.	Dynamic System of Speed Adjustment	4
2.	Silicon Controlled Rectifier (SCR)	6
3.	Single Phase Six Pulse Wave Converter	8
4.	Single Phase Twelve Pulse Wave Converter	9
5.	Static System of Speed Adjustment	11
6.	Darlington Transistor	12
7.	Three Phase Controlled Rectifier and Filter	15
8.	Single Phase Transistor Inverter	17
9.	Single Phase SCR Inverter	19
10.	Three Phase Digital Logic Generator	22
11.	Digital Signal Waveform	24
12.	Rotational Loss vs Speed	30
13.	No-Load Test Data Graph	33
14.	Locked Rotor Test Data Graph	34
15.	Motor Equivalent Circuit	39
16.	Power Out vs Slip (51 hz--186 v)	49
17.	Power Out vs Slip (60 hz--220 v)	50
18.	Power Out vs Slip (75 hz--272 v)	51
19.	Motor Power In vs Slip (20 hz operation)	64
20.	Motor Power In vs Slip (40 hz operation)	65
21.	Motor Power In vs Slip (60 hz operation)	66
22.	Power Out vs Slip (20 hz operation)	67
23.	Power Out vs Slip (40 hz operation)	68

FIGURE PAGE

24. Power Out vs Slip (60 hz operation) 69
25. 60 Cycle Line-To-Neutral Voltage. 71
26. 60 Cycle Line-To-Line Voltage 71
27. 60 Cycle Line Current 71
28. 40 Cycle Line-To-Neutral Voltage. 73
29. 40 Cycle Line-To-Line Voltage 73
30. 40 Cycle Line Current 73
31. 20 Cycle Line-To-Neutral Voltage. 75
32. 20 Cycle Line-To-Line Voltage 75
33. 20 Cycle Line Voltage 75
34. Synthesized Current Waveform--60 hz 78
35. Synthesized Current Waveform--40 hz 79
36. Synthesized Current Waveform--20 hz 80
37. Rectangular Wave and Harmonic Content 85
38. Pulsed Wave and Harmonic Content. 86
39. Solid State Inverter. 101
40. A-C Test Motor and D-C Load Motor 102
41. Complete Test Station 103

CHAPTER I

ADJUSTABLE SPEED ELECTRIC MOTOR SYSTEMS

I. BASIC MOTOR PARAMETERS

The speed of an induction motor can be varied by adjusting any of the following fundamental paramenters: slip, the number of magnetic poles in the motor and the power source frequency. The no-load speed of an induction motor can be determined from the following formula:

$$N_S = \frac{120}{P} \cdot F$$

where N_S = revolutions per minute (synchronous),

P = number of poles,

F = line frequency in cycles per second.

The loaded or slip speed can be determined from the following formula:

$$N_L = (1-S)N_S$$

where N_L = revolutions per minute (loaded),

S = slip.[1]

The following paragraphs will clarify these three parameters.

Some motors (Nema design A, B, and C) have slip which varies typically from 0-5%. For a wound-rotor machine, the speed may be varied in the ratio of four to one through slip

---

[1]Vincent Del Toro, Electromechanical Devices for Energy Conversion and Control Systems (Englewood Cliffs: Prentice-Hall Inc., 1968), p. 169.

control. This speed variance is accomplished by windings in the rotor brought external to the machine by slip-rings and brushes. These rotor windings are then used to load the machine and slow it down. The most common method is using shunt resistors which dissipate energy as heat. More exotic methods use slip power to drive a d-c motor (Kramer drive) and phase shifting of rotor currents to reduce air gap flux. In some slip control procedures, adjustable voltage supplies are used to lower the machine speed. A well designed high-slip high-temperature rotor machine can be speed adjusted in as much as a three to one ratio.

The disadvantage of using slip to vary machine speed is the added complexity of the wound-rotor machine, coupled with the loss of efficiency of both wound-rotor and adjustable voltage drives. High revolutions per minute (rpm) wound-rotor machines are not available because of the mechanical tolerances involved in using slip-rings and brushes with a high speed shaft. The speed of these forms of drive vary drastically with the load. The slip of a synchronous motor will always be zero.

A popular system of speed control is to alter the number of magnetic poles in the motor. This speed adjustment is done with reconnectable stator windings. These winding connections are brought external to the motor allowing the speed to be varied in up to four discreet steps. Characteristic speeds are 1800/1200/900/600 rpm. Frame sizes may or may

not increase for multipole motors. Performance is equivalent to any fixed-pole motor when proper design criteria are followed. These motors are found only in the lower horsepower ratings.

II. DYNAMIC ADJUSTABLE FREQUENCY SYSTEMS

For applications where the previous two methods are not acceptable, the only remaining parameter is power line frequency. The predominant procedure for adjusting line frequency has formerly been the dynamic method. This method involves using a variable speed electric motor to rotate a three phase alternator. An example of the dynamic system is shown in Figure 1. An a-c motor is connected to the alternator through a mechanically-variable speed-changer. The alternator output voltage is adjusted by varying the d-c excitation. Another typical dynamic system uses a d-c motor as the prime mover which is varied by adjusting the d-c motor speed. The dynamic method, although popular for many years, has several distinct disadvantages. The two rotating machines occupy considerable floor space, are expensive to maintain, require a high initial capital expenditure and have a limited operating range. Previously these systems have found applications only where they were mandatory, as in enormously high horsepower single-motor or multi-motor applications.

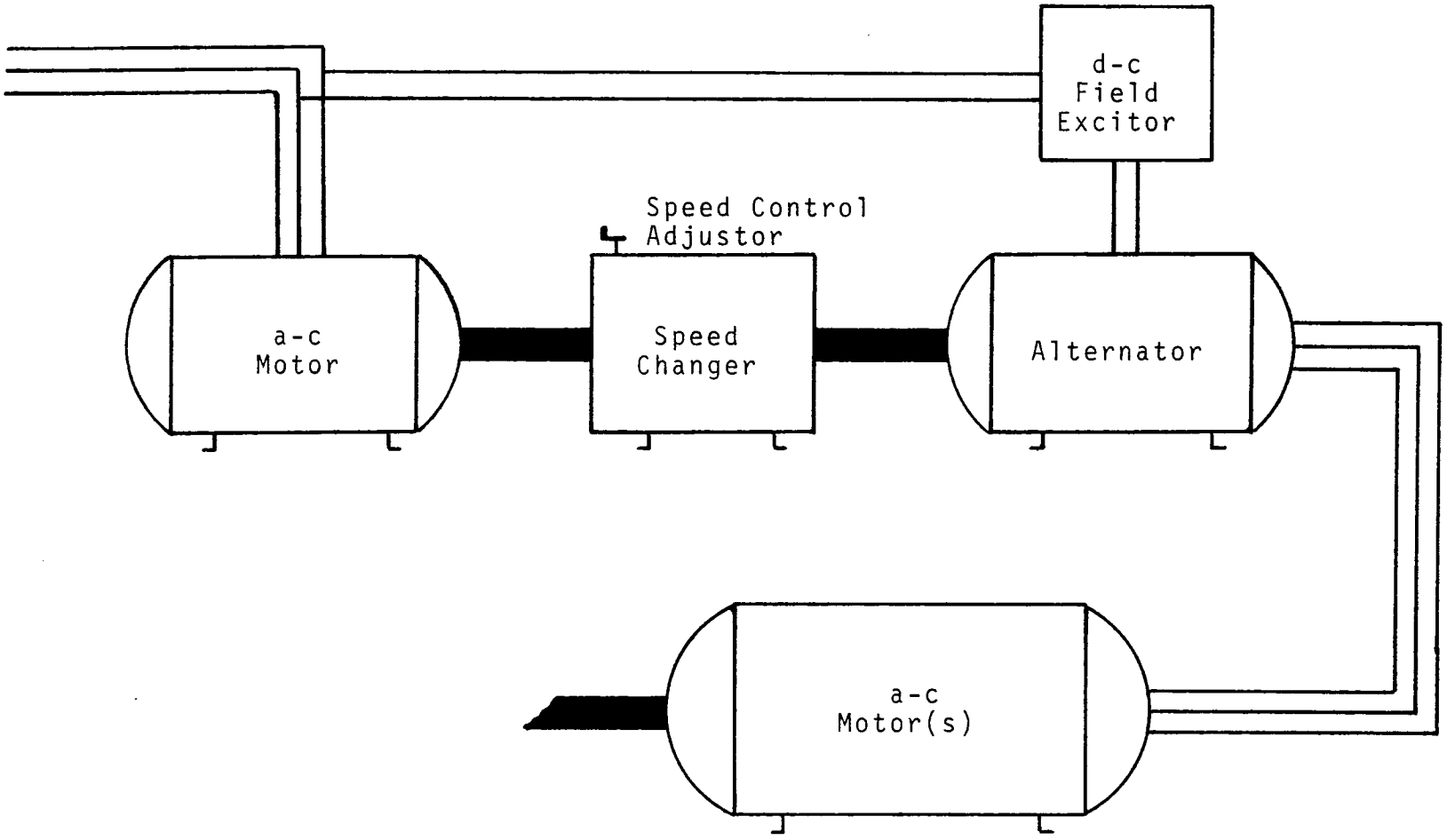

Figure 1. Dynamic System of Speed Adjustment

III. STATIC ADJUSTABLE FREQUENCY SYSTEMS

New designs have incorporated static frequency changers to replace older dynamic systems. The term "static" indicates no moving parts; all the critical machinery has been replaced by solid state electronic devices. Two popular adjustable frequency drives are the cycloconverter, also known as wave-converter, and the rectifier-inverter drive.

Wave-Converter

The earliest application of the wave-converter, or cyclo-converter, was by the German National Railroad in the 1930's. The frequency was stepped down from 50 hertz (hz) to 16 and 2/3 hz. This application was single phase and used thyratron tubes as the power handling device. Modern cycloconverters use sets of silicon controlled rectifiers (thyristors) in series with each of the three a-c lines. Figure 2 shows a diagram of this device. The thyristors are gated to conduct at the proper time to chop the 60 cycle mains to a lower frequency. The quality of the output waveform is dependent on the number of thyristors used to switch the incoming voltage. Since alternating voltage is applied to the anode of the thyristor, commutation can be accomplished by natural means. When the incoming current crosses zero, the thyristor is self-extinguished. Since the input waveform is modified to produce an output waveform, only frequencies of less than 60 cycles are attainable. A practical upper limit on the output fundamental frequency is 1/3 of the input frequency, or 20 cycles.

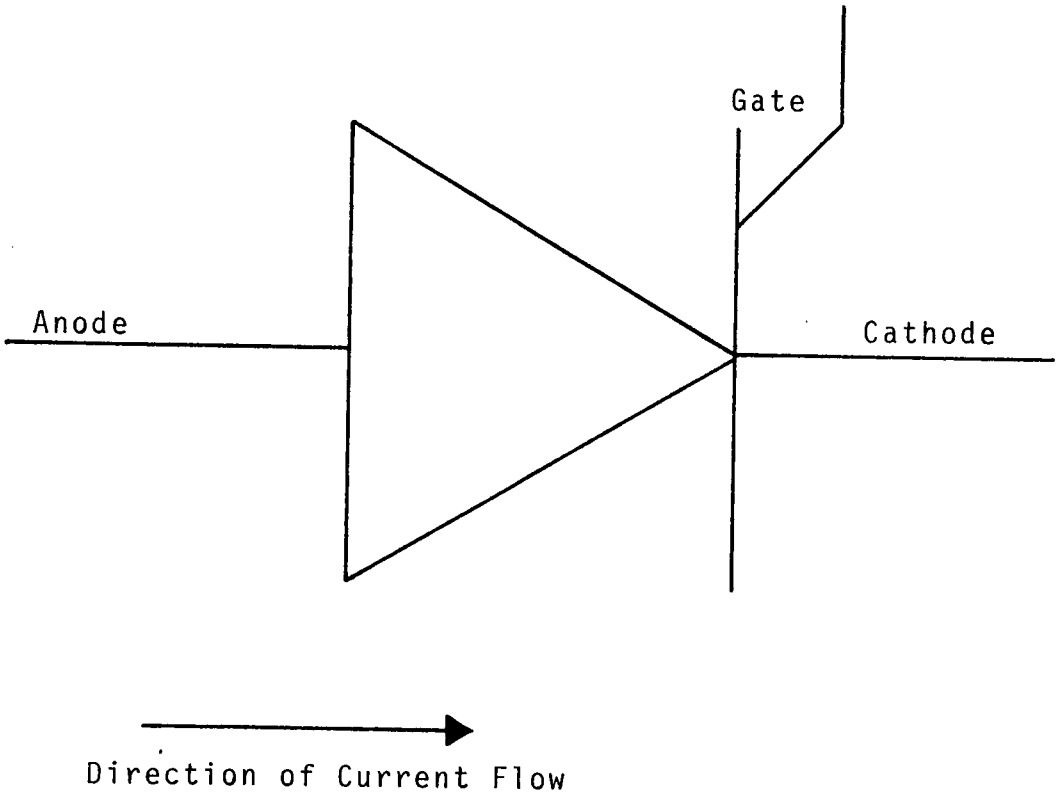

Figure 2. Silicon Controlled Rectifier (SCR)

Cycloconverters are efficient because power is handled only once by semiconductor devices and the output voltage waveform can be improved with more power devices. Figures 3 and 4 show the single phase circuit diagrams of a 6 and 12 pulse converter, respectively.[2] Increased circuit complexity and higher component count go hand in hand with improved waveshape.

The limitation of 20 cycles maximum frequency has restricted cycloconverter usage to applications where high torque and low rpm are necessary. Low speed operation without a preponderance of motor poles is the strong point of this system. The cycloconverter is particularly attractive when the process includes a large, low speed, direct coupled, revolving drum with speed adjustment, accurate or programmable speed control and reversal. Examples of usage are Yankee dryers, friction-type mine hoists, drag lines and attrition mills.[3] All of these applications use either induction or synchronous motors with ratings over 500 horsepower.

Rectifier-Inverter

The last system to be mentioned is the rectifier-inverter drive. This system is capable of frequency ranges from zero to 2000 cycles, and is used in place of cycloconverters

---

[2]B. R. Pelley, Thyristor Phase Controlled Converters and Cycloconverters (New York: Wiley Interscience, 1971), pp. 86-89.

[3]S. J. Campbell, "Static Power Supplies With A-C Machines," Westinghouse Engineer, Volume 32, No. 2 (Pittsburg: Westinghouse Electric Corporation, 1972), p. 36.

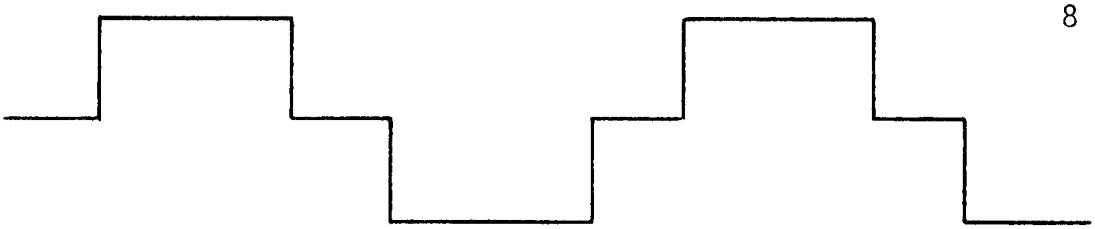

Single Phase Output Waveform

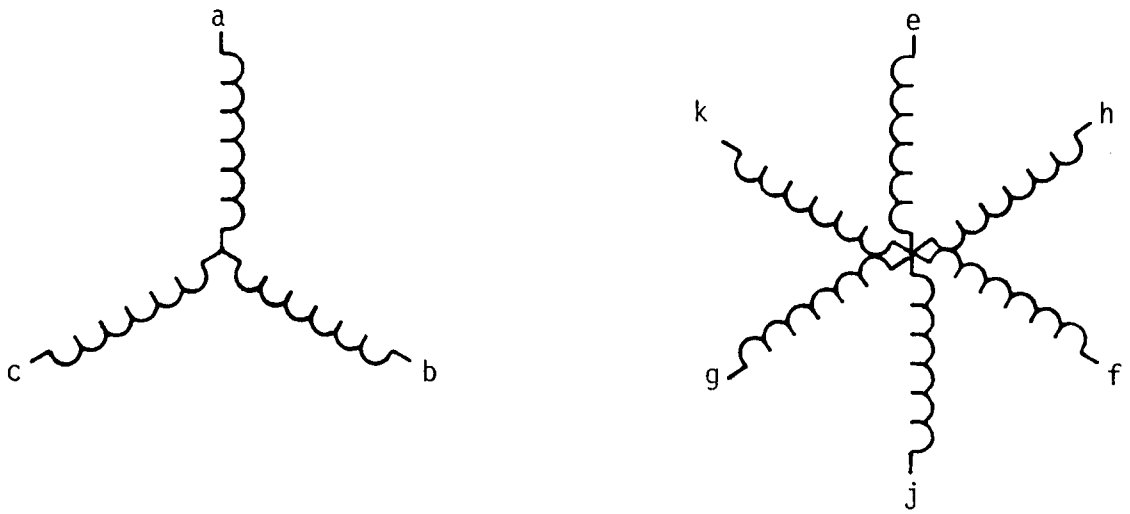

Primary Secondary

Transformer Connections

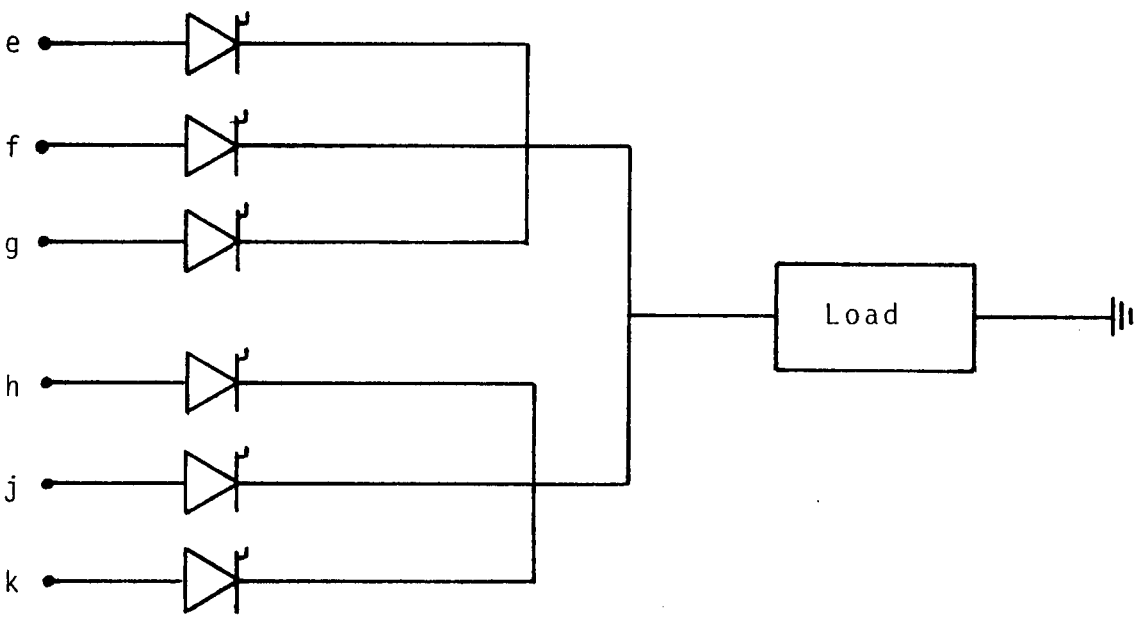

Figure 3. Single Phase Six Pulse Wave Converter

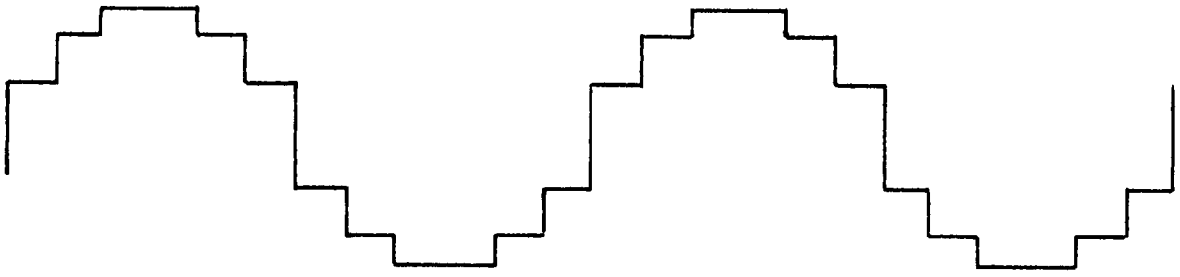

Single Phase Output Waveform

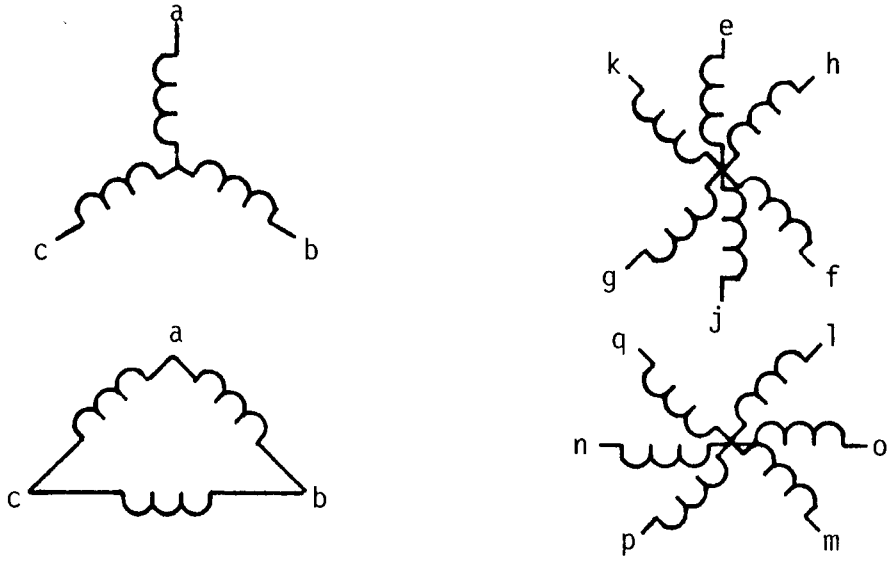

Primary Secondary

Transformer Connections

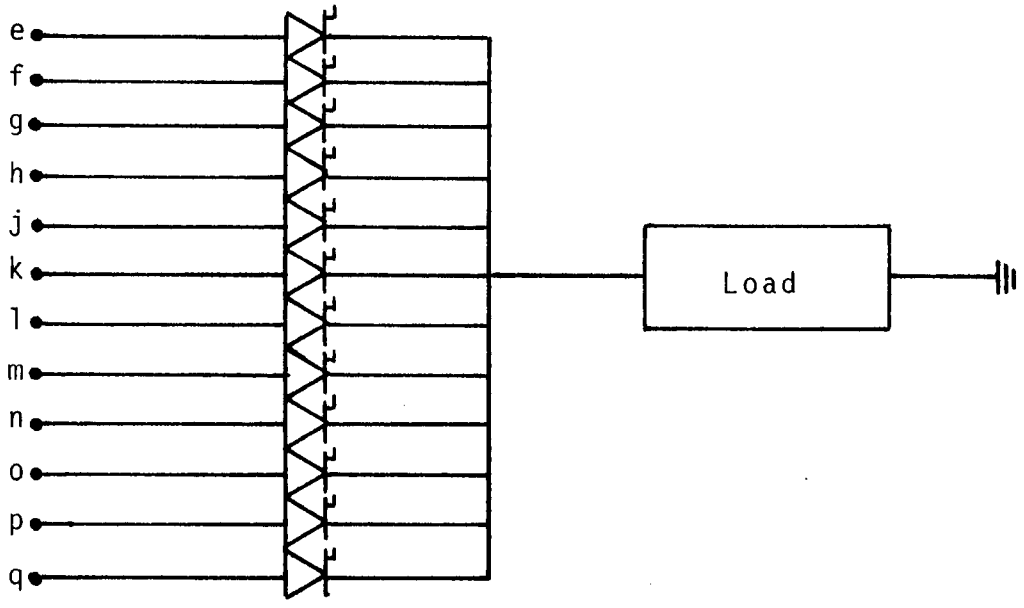

Figure 4. Single Phase Twelve Pulse Wave Converter

where a great speed range is necessary. The typical design has a constant volts/hz operation, preventing machine iron saturation at lower operating frequencies. As shown in Figure 5 the principal functioning blocks of this system are: a controlled rectifier to provide a variable d-c voltage to the inverter section, an inverter section to switch the d-c voltage to the desired output frequency and an oscillator logic section to provide the turn-on signal to the output at the proper time. These functioning blocks are described in greater detail in the next chapter.

The main power handling device for this system can be either a thyristor or a power transistor. Many designs incorporate a particular type of transistor called a Darlington. Figure 6 shows a schematic representation of a Darlington.

The rectifier-inverter drive can be further simplified if a d-c source is used; the d-c source eliminates the rectifier section. Considerable interest has been shown in this type of drive for use in an electric car.[4] The inherent ruggedness, high efficiency and maintainance-free operation of

---

[4]P. D. Agarwal, The GM High Performance Induction Motor Drive Systems (New York: IEEE Trans. Paper No. 68-TP107-PWR, 1969), pp. 86-93; Richard W. Johnston, Modulating Inverter System for Variable Speed Induction Motor Drive (GM Electrovair II)(New York: IEEE Trans. Paper No. 68-TP108-PWR, 1968), pp. 81-85; Jalal T. Salihi, Induction Motor Control Scheme for Battery Powered Electric Car (GM Electrovair I)(New York: IEEE Trans. Paper No. 68-TP22-IGA, 1968), pp. 149-157; Earnest H. Wakefield, An A-C Drive Electric Vehicle (New York: IEEE Trans. Paper No. TOD-73-87, 1973), pp. 544-552.

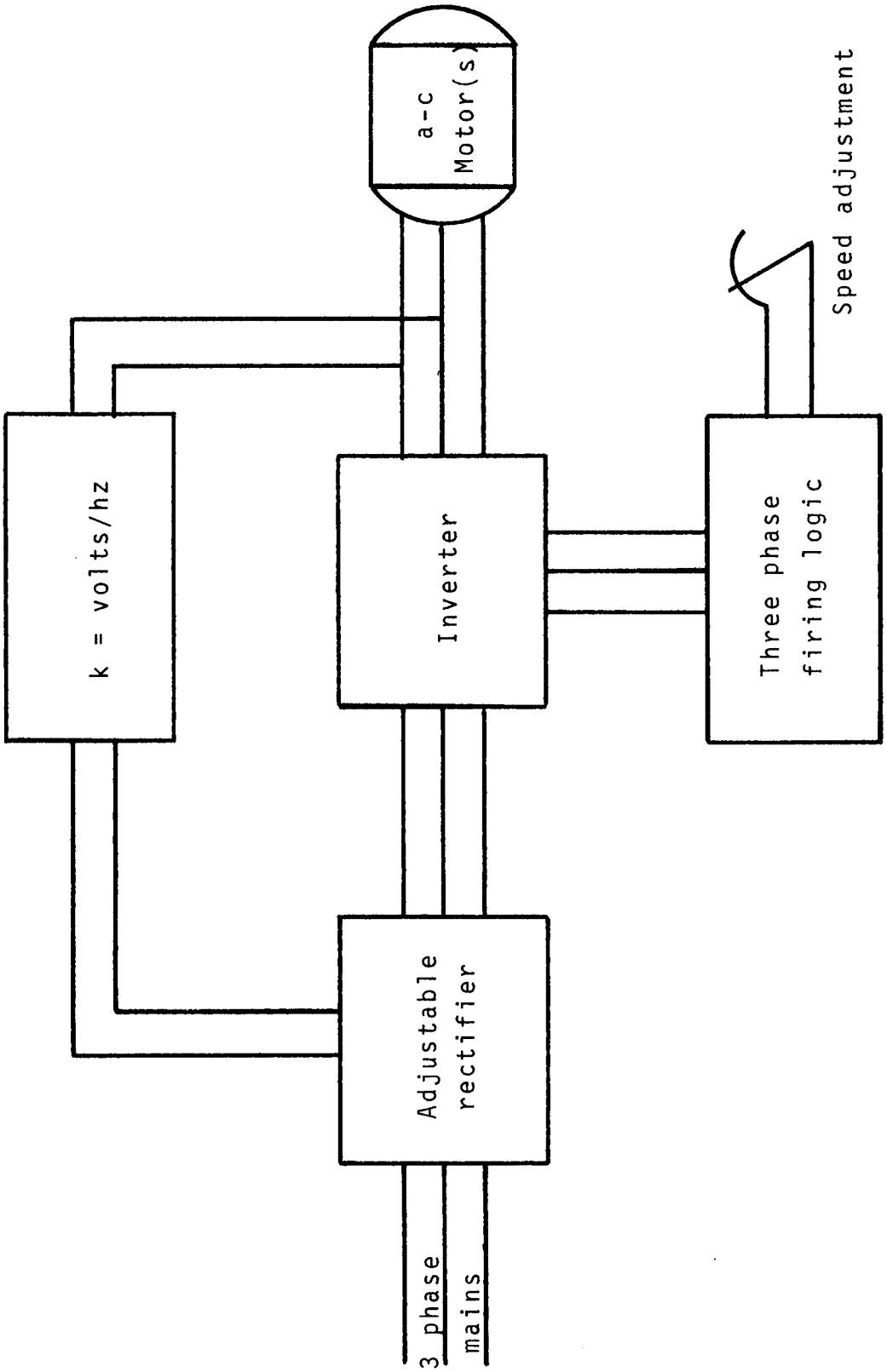

Figure 5. Static System of Speed Adjustment

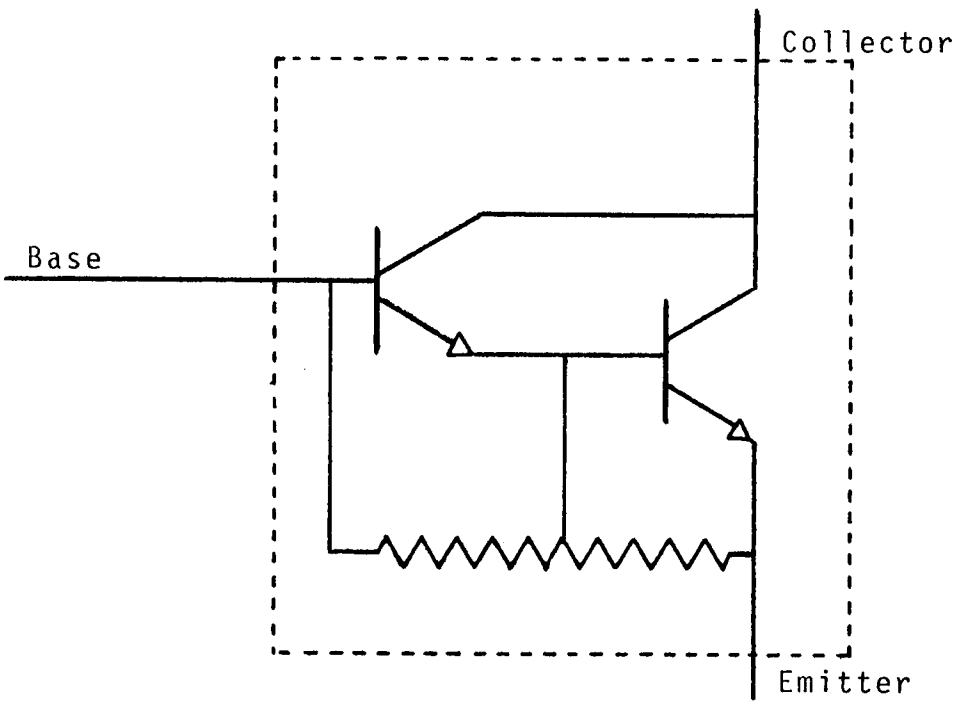

Figure 6. Darlington Transistor

the polyphase induction motor enhances this type of motor drive.

This chapter has analyzed most of the speed control methods for the three phase induction motor. The area to be studied in future chapters will be the rectifier-inverter system. This method holds promise to revolutionize usage of motor speed controls. Employment in a mass produced item such as an electric car would drastically reduce prices. This reduction would open up applications of rectifier-inverter systems which have been previously prohibited because of economic reasons. Thus the main area of investigation in this paper is the rectifier-inverter system and its effects on the performance of the three phase induction motor.

CHAPTER II

THE RECTIFIER-INVERTER SYSTEM

I. THREE PHASE CONTROLLED RECTIFIER

Figure 7 shows a schematic representation of a three phase controlled rectifier. This system is the first functional block of the rectifier-inverter system outlined in Chapter I. As seen on the schematic diagram, six thyristors are used: SCR1, SCR2 and SCR3 for the positive output voltage and SCR4, SCR5 and SCR6 for the negative output voltage. The term "controlled rectifier" indicates the output voltage can be varied over a given range. Controlled conduction is precisely why thyristors are used instead of conventional silicon diodes. In the case of thyristors, maximum output voltage is derived from 120 degree conduction (simple diode operation). The voltage may be reduced by delaying the initial turning on of the thyristor. If the output devices conduct for only 100 degrees, obviously the output voltage will be reduced. The thyristors are self-extinguished when the imput voltage reverse biases the anode-cathode junction.

A filter network; L1, L2, C1 and C2 reduces the output voltage ripple. To improve output voltage waveform, additional stages of filtering may be included. It is not uncommon for the designer to fuse the B+ and B- lines to isolate functional blocks in case of failure.

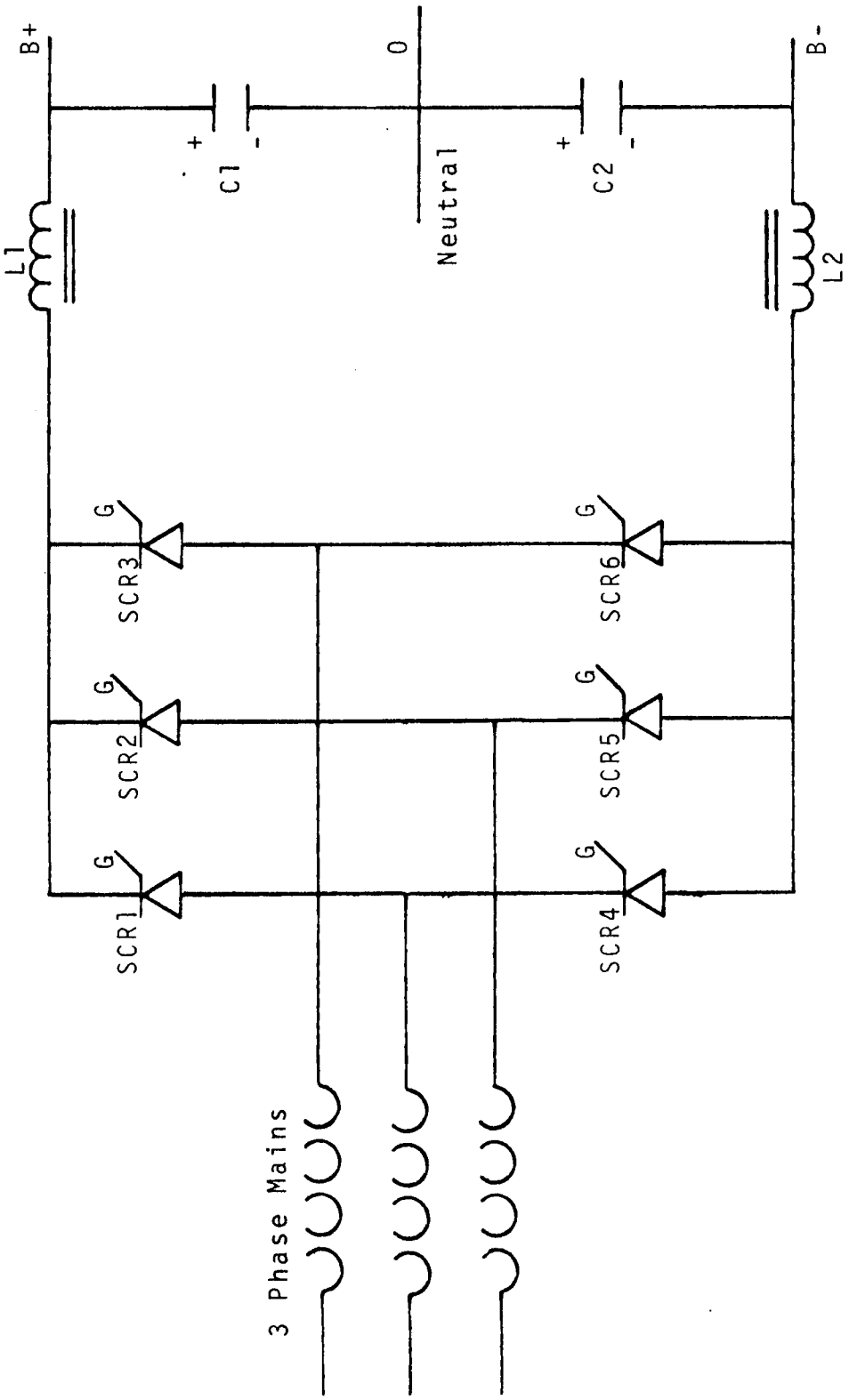

Figure 7. Three Phase Controlled Rectifier and Filter

II. TRANSISTOR INVERTER

The circuit in Figure 8 uses power Darlington transistors Q1 and Q2 to conduct power to the load during alternate half-cycles. Feedback diodes D1 and D2 feed reactive power from the load back to the d-c supplies, while their parallel power transistor is non-conducting. The transistor conducting at any given time must have the base signal present during conduction. The signal must be of sufficient magnitude to cause the Darlington to operate as a saturated switch. Non-saturated operation can generate enough junction heat to cause early failures. Many systems utilize protective circuitry to insure that the transistor last conducting has been completely shut down prior to bringing conduction up on the next transistor. This protection prevents a "fire through" condition, where B+ is connected to B- through the series conducting devices Q1 and Q2. Conduction time of this system can be continuously adjusted on the half-cycle from 0 to almost 180 degrees, depending on the complexity of the signal generating system.

An RC snubber network is connected across each power transistor. These networks share load current while the transistor is turning off, and slow the emitter voltage rise while energy is still flowing out of the emitter. This load sharing reduces electrical stress on the power devices. Capacitor C determines the turn-off Vce rising slope. Resistor R limits the capacitor discharge current through the

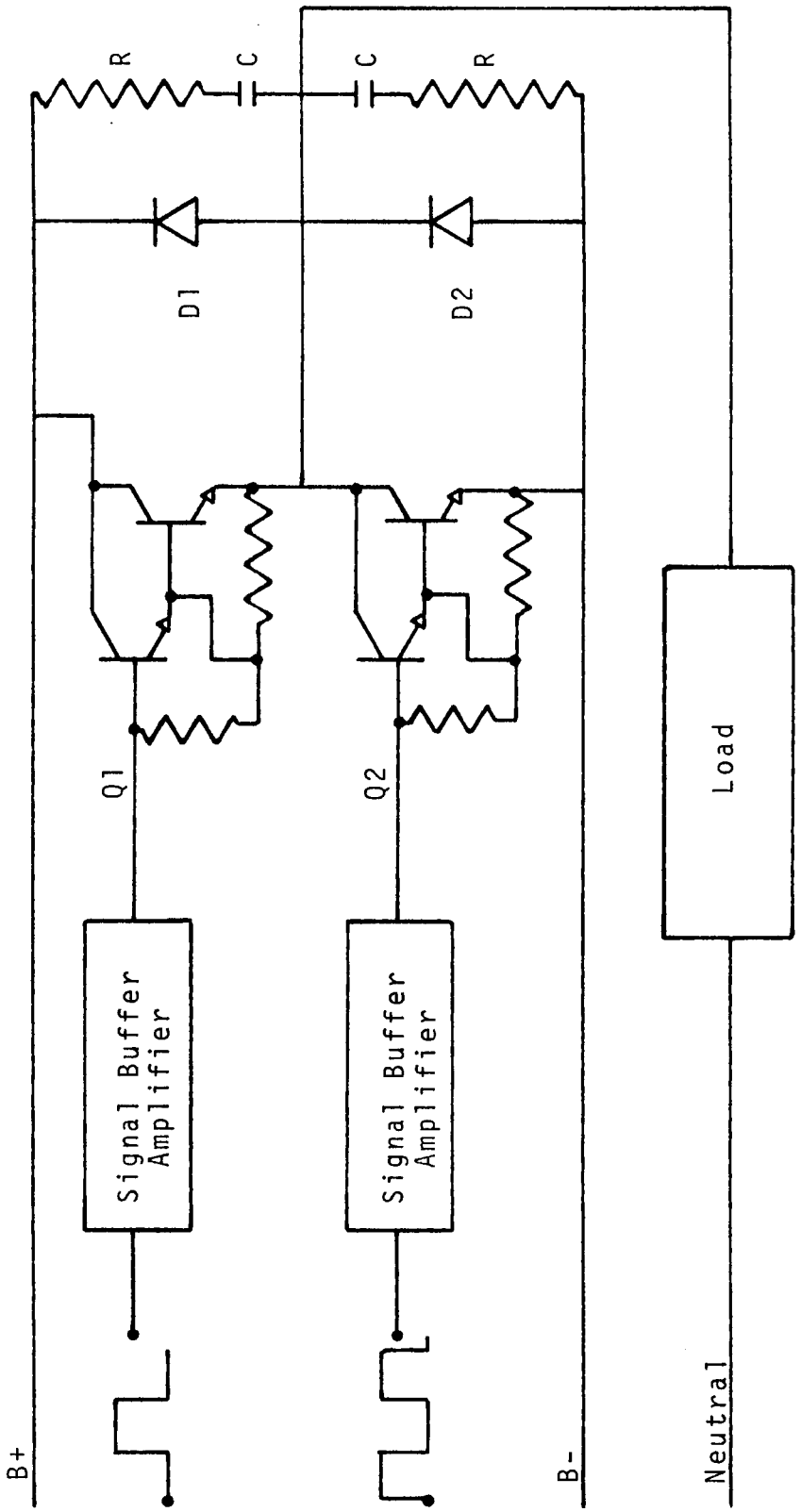

Figure 8. Single Phase Transistor Inverter

transistor during turn-on. A typical set of values is R=10 ohms and C=.5 micro farads.

Increased power can be delivered to the load by adding output devices in parallel. The current will divide equally between them. Companies such as Ramsey Controls, Precision Transformer and Parajust have transistorized motor controls in their product lines. Because of the relative fragility of the transistor, this type of design is limited to motor drives of 10 horsepower or less. In the lower power applications however, the transistor presents a definite economic advantage over the thyristor.

In this single phase example, two base drive pulses are required for operation. They are inverses of each other and vary in duty cycle according to desired output power. Because of the low current gain of the Darlingtons they may be as high as 250 ma to switch 1 amp. The maximum frequency of operation is limited primarily by the turn-on and turn-off time of the power devices.

III. SILICON CONTROLLED RECTIFIER-INVERTER

The circuit of Figure 9 uses primary controlled rectifiers SCR1 and SCR2 to conduct power to the load during alternate half-cycles. For a leading or lagging power factor the feedback diodes D1 and D2 conduct, during segments of alternate half-cycles, to return stored power from the load to the supply. Unlike power transistors, when the thyristor is

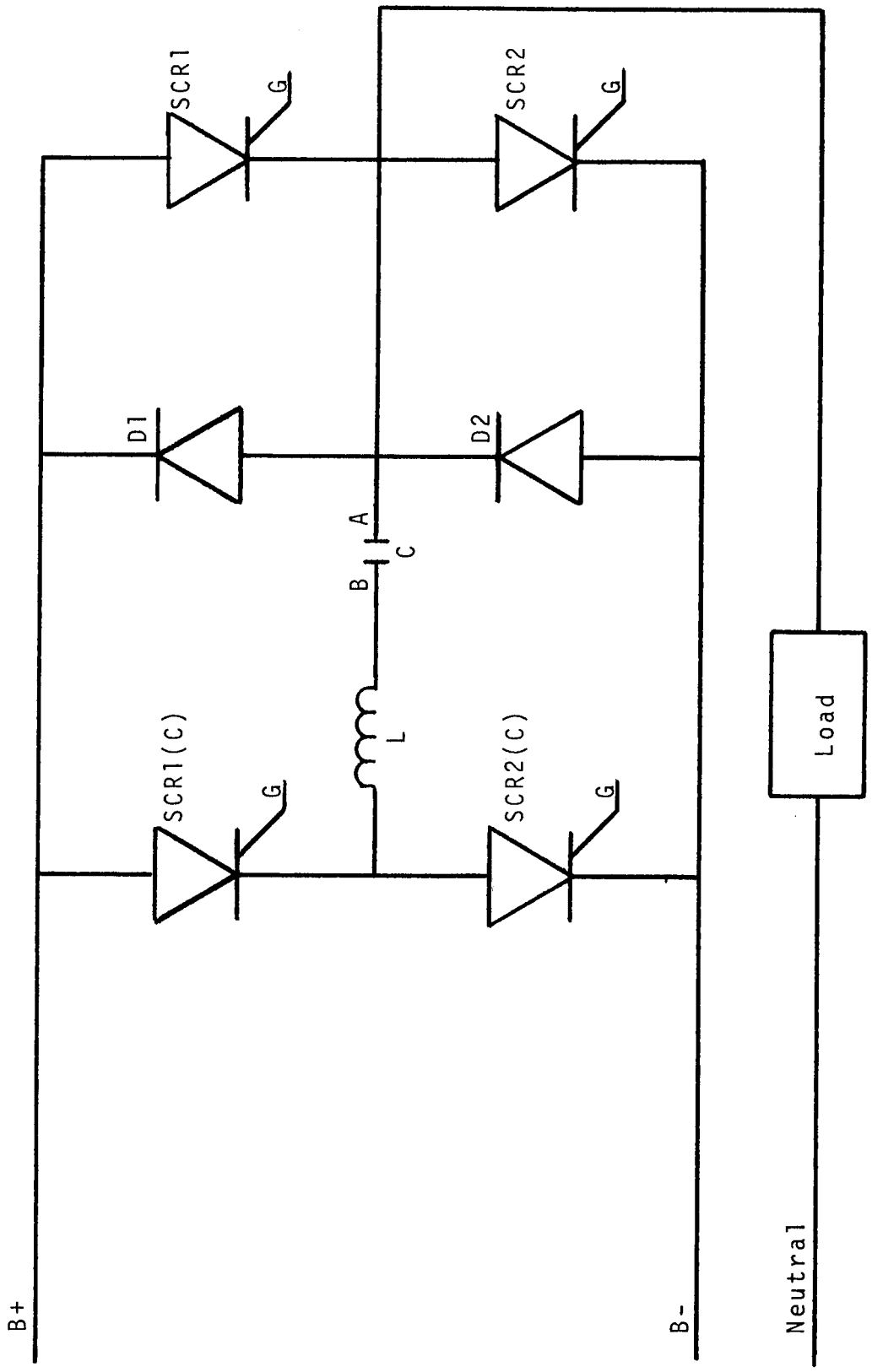

Figure 9. Single Phase SCR Inverter

gated on it continues to conduct until the anode current is reduced to zero. This process is called commutation. The gate turn-on pulse can be a very low energy pulse of short duration. The primary controlled rectifiers are extinguished through the firing of the commutation controlled rectifiers SCR1-C or SCR2-C. This conduction path, in conjunction with the LC network, generates the proper extinguishing pulse.

To analyze one complete cycle of operation, assume SCR1 is conducting and all other semiconductors non-conducting. A positive voltage is applied to the load, and capacitor C is charged with A positive with respect to B. To shut off SCR1, SCR1-C is fired, bringing point B on C to approximately B+, and point A on C to about 2B+. Now the cathode of SCR1 is positive with respect to the anode and current will cease to flow. Excess commutation current stored in the LC network is returned to the positive supply through the feedback diode D1. At approximately the same time that D1 has drained off the energy in LC, SCR2 is fired. The load now sees a negative voltage and point A is charged negative with respect to point B. This reversing of C voltage commutates SCR1-C. With SCR2 conducting, all other semiconductors non-conducting, and C charged B+ with respect to A, SCR2 can be commutated by firing SCR2-A. This conduction path develops a voltage of B- bias condition on SCR2, reducing its current to zero. Diode D2 is forward biased discharging LC. Gating SCR1 on finishes one cycle of the operation. A snubber

network consisting of a resistor and capacitor is normally placed across each power handling SCR to prevent voltage transients during turn-on.

In this single phase example, four firing pulses of different duration and phase are applied to the gates of the SCR's. It is the periodicity of these gate signals which determines the fundamental frequency of current to the load. Minimum and maximum frequency of operation are limited primarily by turn-on and turn-off time of the SCR's.

IV. THREE PHASE DIGITAL LOGIC

The last functional block of the static adjustable speed system is the three phase firing logic circuit. An example of this system is shown in Figure 10. This circuit generates three output voltages each a symmetrical square wave, phase shifted 120 degrees with respect to each other. The input signal is obtained from a voltage controlled oscillator LM 566. The frequency is adjustable from 84 to 840 hz by shifting the d-c voltage to pin 5 of the VCO via a potentiometer. The input signal is first divided by two in IC2-A giving logic levels compatable with the rest of the circuit. The output of IC2-A is then used as the clock pulse for the three sequentially connected bistables IC2-B, IC3-A and IC3-B. The first bistable, IC2-B, derives its inputs from the NAND gates, whose final output is shifted every other clock pulse. Output I is the positive (Q) output of IC3-B. Output II is

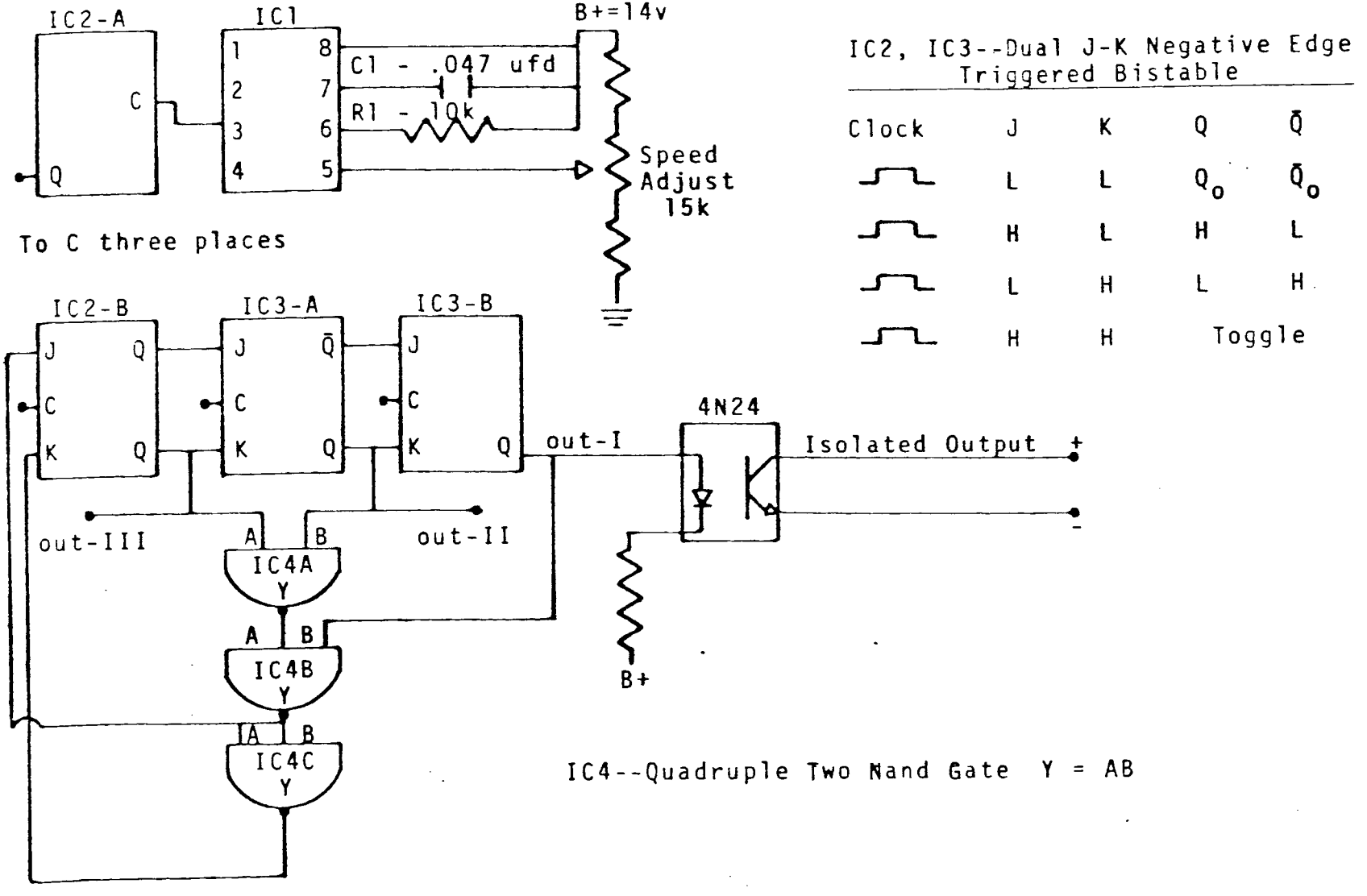

Figure 10. Three Phase Digital Logic Generator

the negative input of IC3-B, making output I the inverse of output II plus one clock pulse. Therefore:

output I = -output II + 60 degrees,

or

output I = output II + 120 degrees.

Similarly, output III is shifted 120 degrees from the other two outputs. The final output frequency is adjustable from 7 hz to 70 hz. Figure 11 shows an oscilloscope trace of the three outputs.

Output I is shown in series with an optical isolation device. This device has superseded transformers in many applications where differential ground potentials exist. A photon-coupled isolator such as the 4N24 has a voltage isolation of $\pm$1 KV with rise and fall times in the microsecond region.

Future developments in integrated circuit technology will lead to a complete controller in a single package. This package could have provisions for any type of control imaginable. Mass production for the industrial market will result in low prices for these devices.

This chapter has discussed several of the main functional blocks of the rectifier-inverter system. There have been many simplifications to provide general information. Unlimited variations of these basic circuits are currently in use to provide power to particular load applications. Methods such as pulse width modulation and harmonic filtering reduce

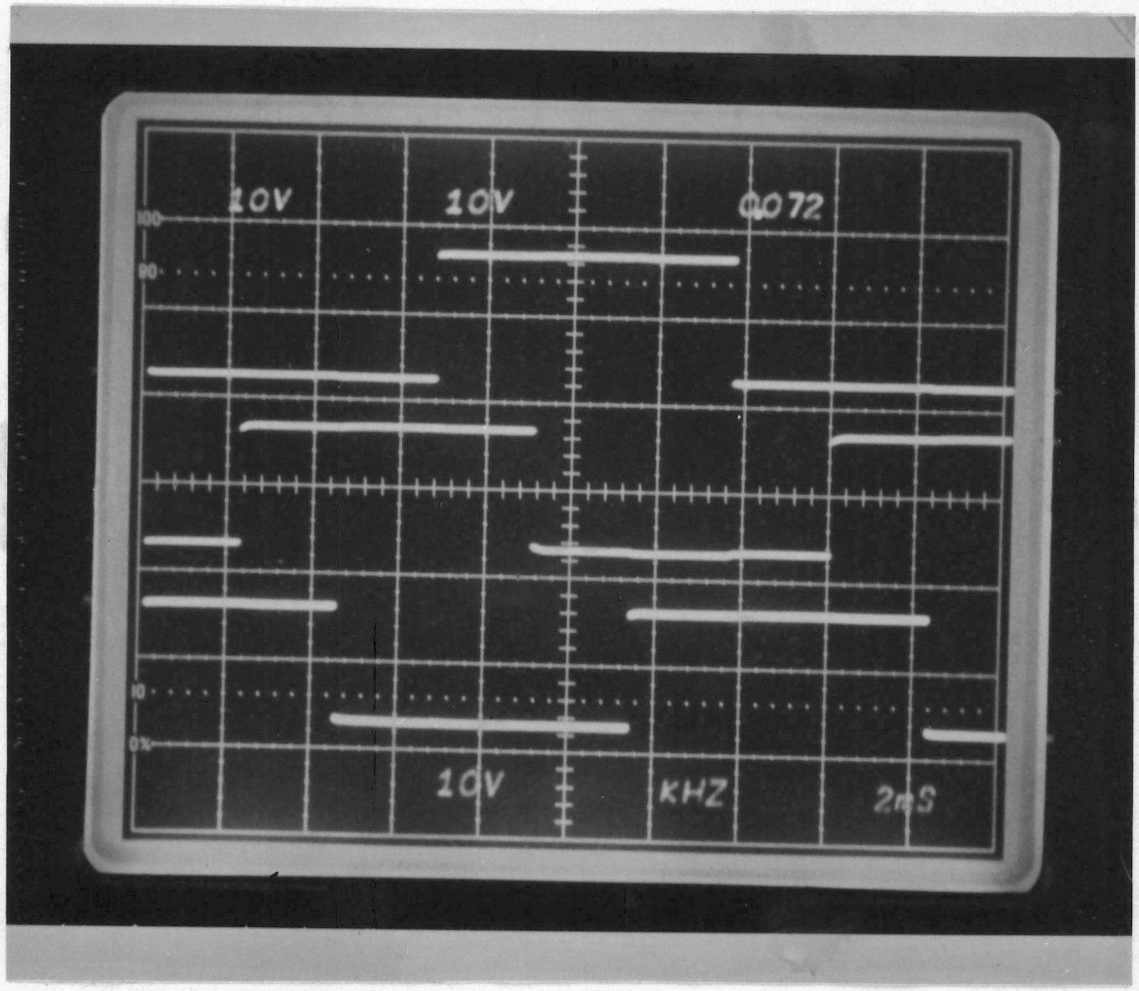

Figure 11. Digital Signal Waveform

unwanted high frequency current to the load. Returning braking power to the energy source further complicates both the inverter and rectifier circuits. Systems with these additions would each have to be analyzed on an individual basis. A general characteristic of these drives is a constant volts/hz operation, preventing machine iron saturation due to higher current flow at lower frequencies. At the extreme lower end of frequency range, this ratio may be increased to compensate for motor IR drop.

CHAPTER III

MOTOR PERFORMANCE CALCULATIONS--SINUSOIDAL VOLTAGE SOURCE

To study the effects of a solid state inverter on an induction motor, a motor must first be analyzed completely to form a basis of comparison. This analysis involved development of the motor equivalent circuit. The equivalent circuit was developed from the locked-rotor and no-load tests. Calculated values and data obtained from actual loading tests were compared to check the validity of this method of analysis. To check the frequency dependent parameters of the equivalent circuit, the motor was operated from a dynamic inverter at two different line frequencies. The frequency dependent parameters of the motor equivalent circuit were adjusted to these new frequencies and experimental data compared with calculated data.

I. EXPERIMENTAL PROCEDURES

Great care was taken to instrument the parameters measured. In this manner readings taken could be reproduced, if the same conditions were made to exist again. Specifically:

1. Data taken involving motor rotation were the average of clockwise and counterclockwise rotation.
2. Current and voltage readings were the average of the three lines.

3. Motor speed was read using a strobe with an electronic pulse counter connected to the trigger output.
4. All data was taken after a minimum of thirty minutes warm up time.
5. The machines were properly lubricated throughout the experimental process.

The system of units used were rationalized M-K-S units. All power calculations were recorded in watts. When applicable, graphical results show calculated values as a solid line, experimental values as points. Data in calculations were carried to enough significant digits to insure few rounding errors.

II. ROTATIONAL LOSSES

Rotational losses consist of frictional losses and windage losses. In lower horsepower motors, rotational losses comprise a significant portion of the energy expended. To predict these losses, the motor in question was rotated using an adjustable speed d-c motor. The developed torque and speed of the d-c motor were recorded. Rotational losses were calculated by using the following relationship:

$$\text{Power} = \frac{2\pi nT}{44752} \text{ hp} \qquad \text{where}$$

n = speed (rpm),

T = torque (newton · meters).

The mechanical power expended can be converted to electrical

power units using the following identity:

1 horsepower = 746 watts.

Table I lists experimental data taken for various speeds and the resulting power losses. A graph of the data from Table I is shown in Figure 12. The rotational power loss was the sum of frictional losses and windage losses. These two losses were dependent on frequency in the following manner:

$$P_{f'+w} = K_1(\text{speed}) + K_2(\text{speed})^3 \quad \text{where}$$

$P_{f'+w}$ = bearing friction and windage losses,

K_1 = coefficient of friction loss

K_2 = coefficient of windage loss.[5]

As shown in Figure 12, the windage losses are a significant portion of potential losses. Performance calculations done later will refer to Figure 12 to fix values of rotational losses at particular speeds.

III. EQUIVALENT CIRCUIT CALCULATIONS

No-load test data and locked-rotor test data are given in Tables II and III. A graphical representation of these experiments is given in Figures 13 and 14. Test procedures, methods of calculation and formulae are taken predominately from the IEEE Standards.[6]

---

[5]Henry R. Reed, Electrical Engineering Experiments (New York: John Wiley and Sons, Inc., 1948), p. 167.

[6]Test Procedure for Polyphase Induction Motors and Generators (New York: The Institute of Electronics Engineers, Inc., 1964), pp. 5-21.

TABLE I. ROTATIONAL LOSS DATA

Point	Speed (rpm)	Force (n)	Torque (n·m)	Power Loss (watts)
1	700	2.54	.355	26
2	1000	2.89	.404	42
3	1200	4.00	.559	70
4	1600	4.45	.622	104
5	2000	5.56	.777	163
6	2400	6.00	.840	211
7	2600	6.23	.870	237
8	2800	6.45	.901	264
9	3000	6.89	.963	303
10	3200	7.12	.995	333

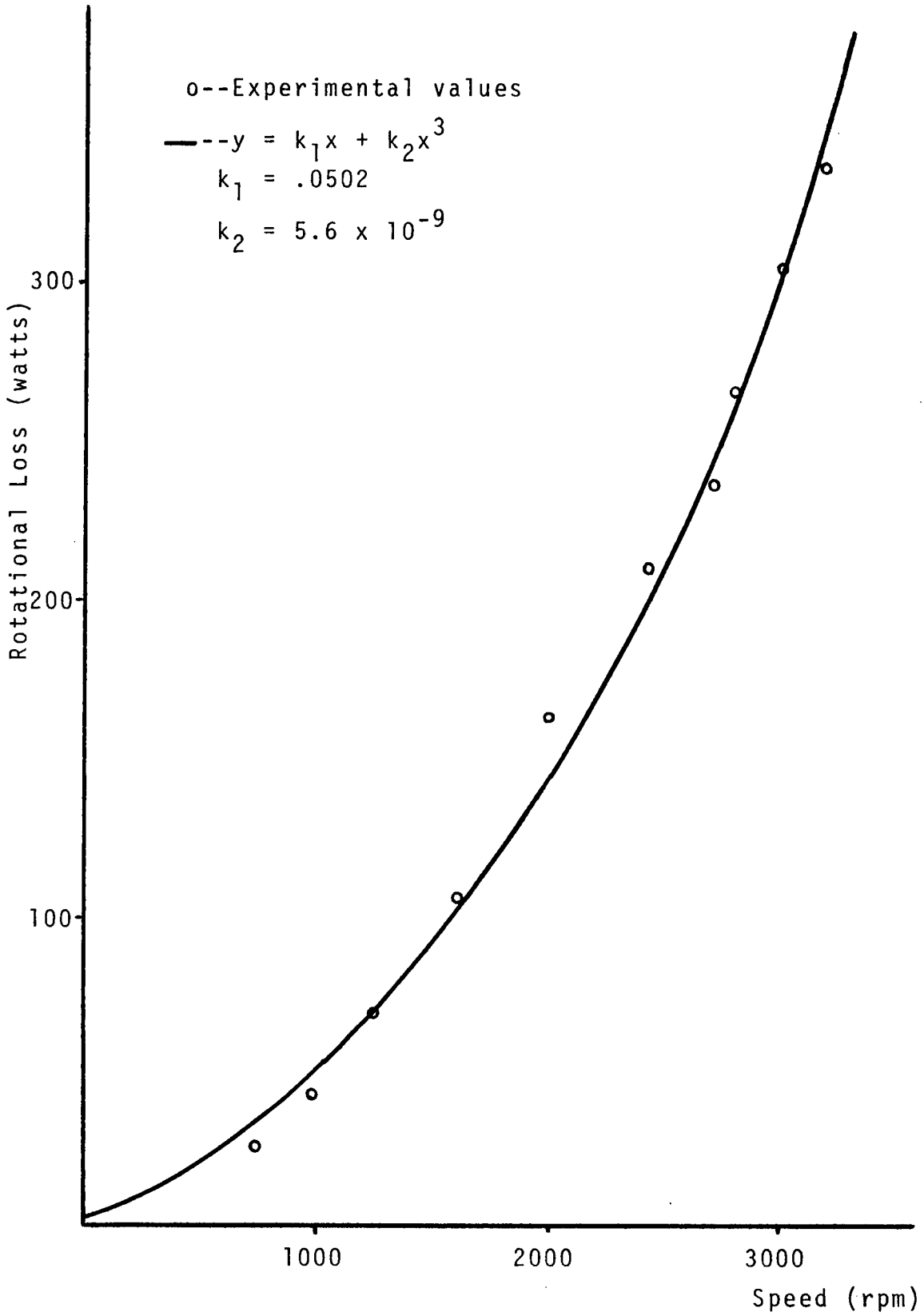

Figure 12. Rotational Loss vs Speed

TABLE II. NO-LOAD TEST DATA

Point	Input Voltage (l-l)	Current (a)	Power (w)	Speed (rpm)
1	239	1.38	230	1786
2	220	1.25	215	1785
3	200	1.15	204	1781
4	180	1.10	193	1776
5	160	1.05	184	1773
6	140	1.03	176	1763
7	120	1.05	170	1758
8	100	1.20	174	1717
9	80	1.60	180	1632

TABLE III. LOCKED ROTOR TEST DATA

Point	Voltage (l-l)	Current (a)	Power (w)	Torque (n.m)
1	44	1.5	44	
2	54	2.0	84	.124
3	64	2.5	130	.248
4	73	3.0	195	.310
5	83	3.5	270	.435
6	92	4.0	354	.559
7	102	4.5	452	.621

D-C stator resistance (hot) -4.95 ohms/phase.

Nameplate Specifications:

Century Electric Co., 3/4 hp, 3 phase, 220 volts, 1800 rpm, .05 slip at rated load, type SC, Frame SOM 1 1/2 BSBB, Spec. #2630.

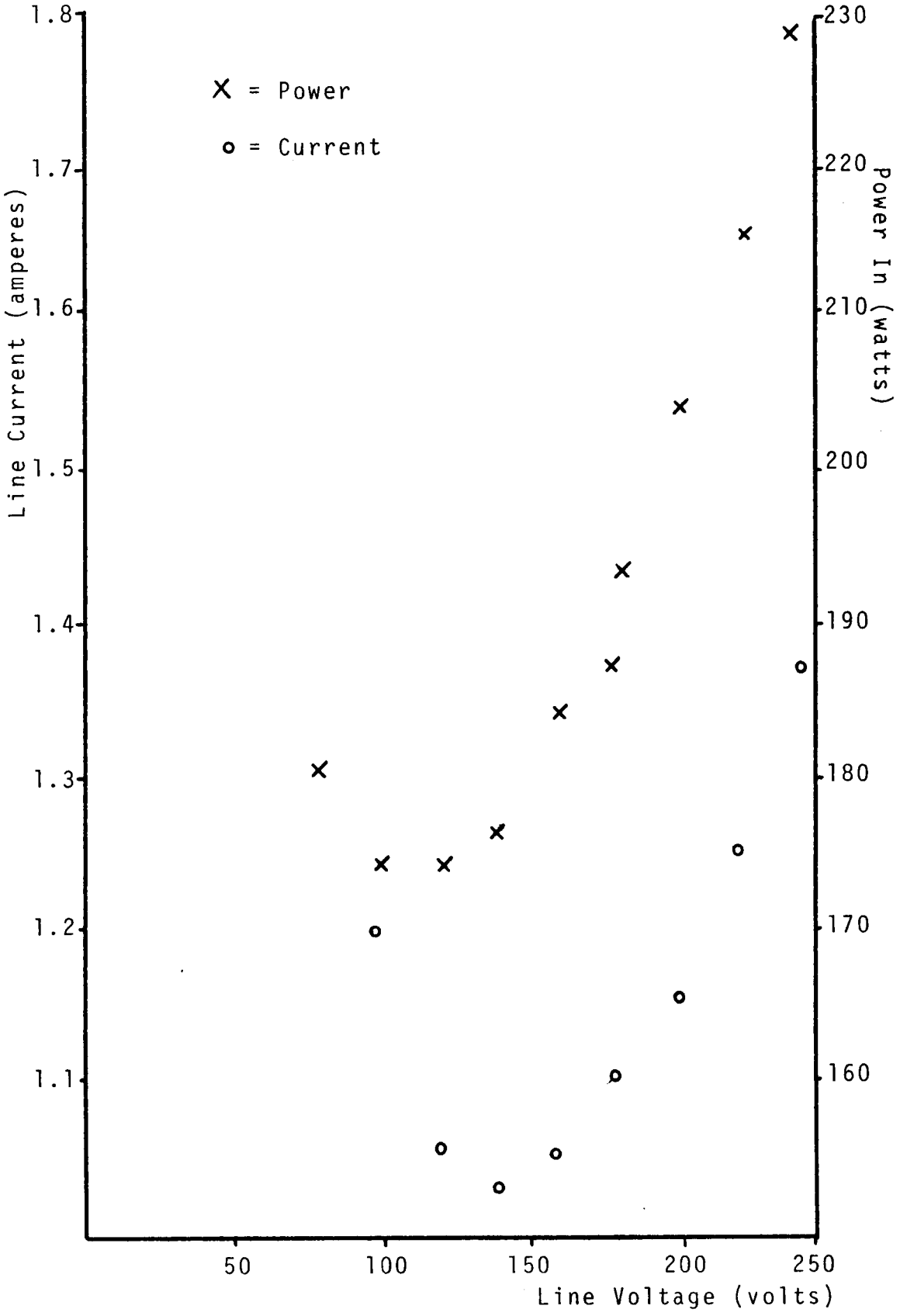

Figure 13. No-Load Test Data Graph

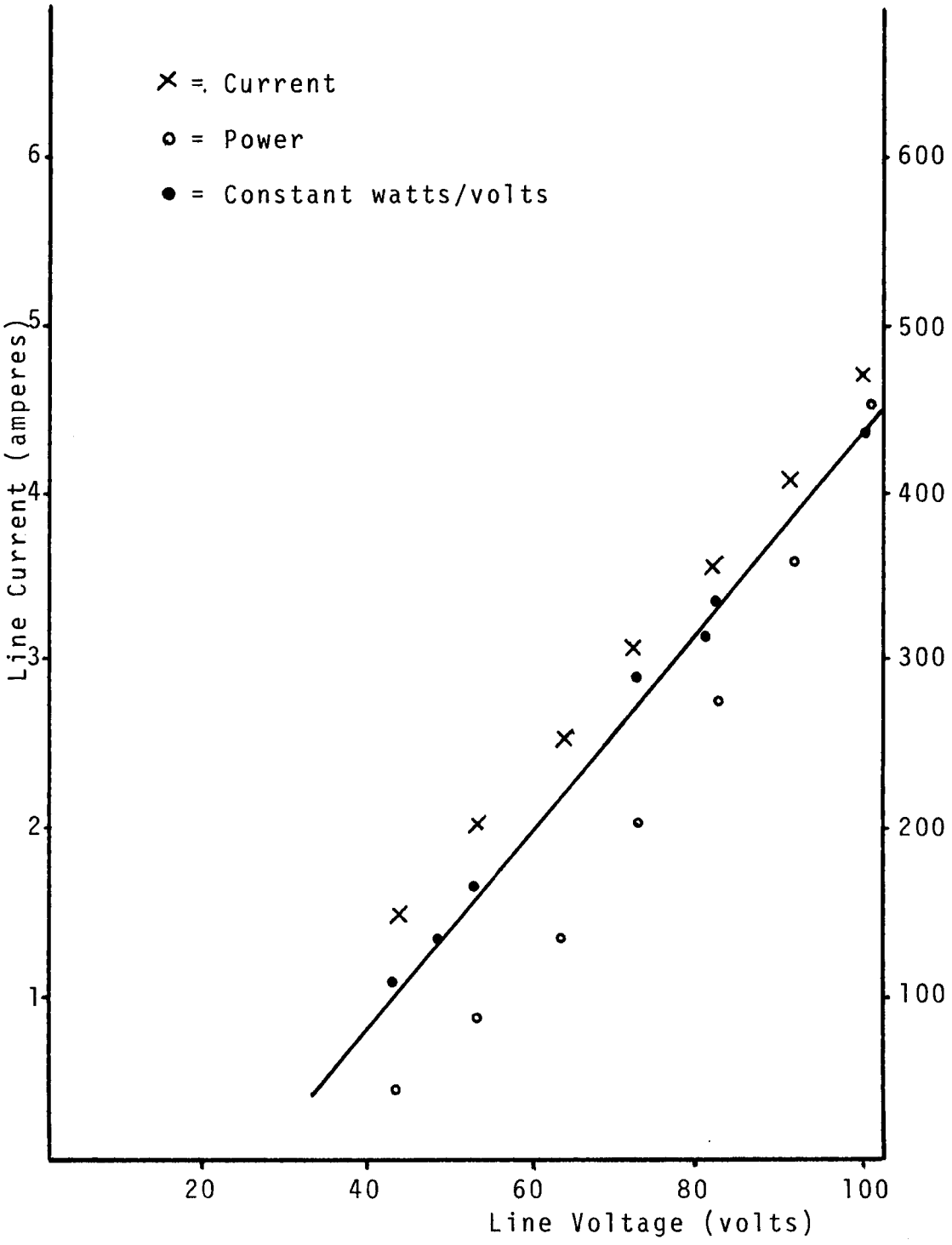

Figure 14. Locked Rotor Test Data Graph

From the locked rotor test, choosing a line current near maximum rated load:

$$x_1 + x_2 = \sqrt{\frac{V_{1r}^2}{3I_{1r}^2} - \left(\frac{W_{1r}}{3I_{1r}^2}\right)^2}$$

$$x_1 + x_2 = \sqrt{\frac{73^2}{3(3)^2} - \left(\frac{195}{3(3)^2}\right)^2}$$

$$x_1 + x_2 = 12 \text{ ohms.}$$

For design A motors:

$$x_1 = x_2$$

thus,

$$x_1 = x_2 = 6 \text{ ohms.}$$

$$R_2 = \frac{W_{1r}}{3I_{1r}^2} - R_1$$

$$R_2 = \frac{195}{3(3)^2} - 4.95 = 2.27 \text{ ohms.}$$

No-load data were used to calculate circuit values for the magnetizing circuit. The data set for rated line voltage was used. Calculations were made on a per phase basis. Let:

I_c = core loss current,

I_{lr} = locked-rotor current,

I_{nl} = no-load current,

R_m = core loss resistor,

X_m = magnetizing reactance,

V_1 = stator voltage,

V_2 = rotor voltage,

V_{lr} = locked rotor input voltage,

W_c = core loss power--hysteresis and eddy-current,

W_{lr} = locked-rotor input power,

W_{nl} = no-load input power,

W_{rw} = rotational losses,

W_s = stator copper loss.

Stator copper loss:

$$W_s = I_{nl}^2 R_1,$$

$$W_s = (1.25)^2 (4.95)$$

$$W_s = 8 \text{ watts}.$$

Core loss power:

$$W_c = \frac{W_{nl}}{3} - W_{rw} - W_s.$$

Rotational loss, taken from Figure 12, was 135 watts or 45 watts per phase:

$$W_c = \frac{215}{3} - 45 - 8 = 19 \text{ watts.}$$

Rotor input voltage:

$$V_2 = V_1 - I_1\sqrt{R_1^2 + X_1^2}$$

A slightly higher value of I_1 was used to compensate for reduced stator input voltage at higher loads.

$$V_2 = 127 - 1.8\sqrt{(4.95)^2 + (6.0)^2}$$

$$V_2 = 113 \text{ volts.}$$

Core loss current:

$$I_c = \frac{W_c}{V_2}$$

$$I_c = \frac{19}{113} = .168 \text{ amperes.}$$

Core loss resistor:

$$R_m = \frac{V_2}{I_c}$$

$$R_m = \frac{113}{.168} = 673 \text{ ohms.}$$

Core loss conductance:

$$G_m = \frac{1}{R_m}$$

$$G_m = .001487 \text{ mhos.}$$

Magnetizing reactance:

$$X_m = \frac{E_1}{I_{n1}} - X_1$$

$$X_m = \frac{127}{1.25} - 6.0 = 95.6 \text{ ohms.}$$

Magnetizing susceptance:

$$B_m = \frac{1}{X_m}$$

$$B_m = .01046 \text{ mhos.}$$

Figure 15 shows the completed equivalent circuit with all component values indicated. Frequency dependent components, X_1, X_2, X_m have their values shown for the three operating frequencies for which performance will be calculated in this chapter.

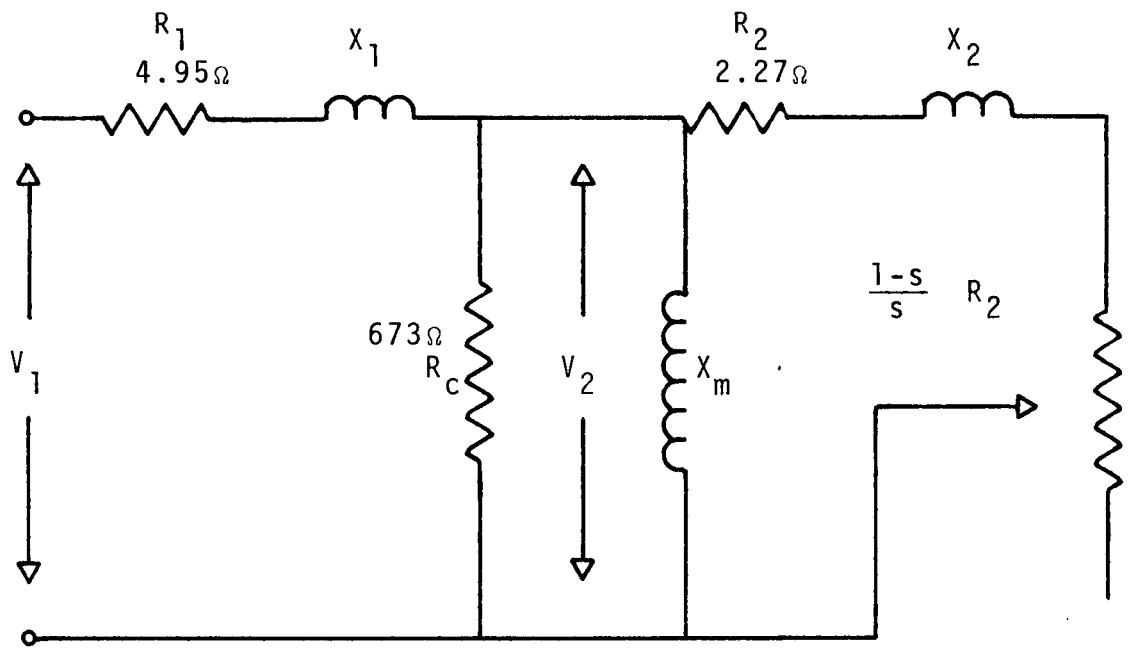

Frequency	$X_1 = X_2$	X_m	V_1
51.1 hz	5.16Ω	82.2Ω	107.4 v
60.0	6.00	95.6	127.0
75.1	7.50	119.6	157.0

Figure 15. Motor Equivalent Circuit

IV. PERFORMANCE CALCULATIONS UNDER LOADED CONDITIONS

To check experimental values, the equivalent circuit was solved completely for six values of slip. The resulting data were used to construct a graph upon which experimental values and calculated values can be compared. Tables IV, V and VI are an organized progression of the algebraic manipulations necessary to solve the equivalent circuit. Proper adjustment of the frequency dependent parameters is all that is needed to calculate performance at various line frequencies.

Each line on the above mentioned tables represents at least one mathematical operation. A more detailed explanation of each line is as follows:

1. $\text{Slip} = \dfrac{\text{synchronous speed - actual speed}}{\text{synchronous speed}}$.

2. $Z_2 = \sqrt{\dfrac{R_2^2}{S} + x_2^2}$ values for R_2 and x_2 are taken from the equivalent circuit.

3. and 4. Per phase input impedance - $R_o + jx_o$,

$$G - jB = \frac{R_2}{sZ_2^2} - j\frac{x_2}{Z_2^2} + G_m - jB_m$$

$$Y = \sqrt{G^2 + B^2}$$

$$R + jx = \frac{G}{Y^2} + j\frac{B}{Y^2}$$

TABLE IV. PERFORMANCE CALCULATIONS (51 HZ, 186 VOLTS)

Line No.	Description	Load Points 1	2	3	4	5	6
1	Slip	1.0	2.0	2.5	3.0	4.0	5.0
2	Z_2	227.1	113.6	90.9	75.8	57.0	45.7
3	R_o	36.8	44.0	44.0	43.0	39.5	35.8
4	jX_o	j71.4	j52.8	j45.3	j39.2	j30.3	j24.6
5	Z_o	80.3	68.7	63.14	58.09	49.78	43.4
6	P.F.	.4577	.64	.697	.74	.794	.824
7	I_1	1.34	1.56	1.70	1.85	2.16	2.48
8	W_i	197	322	382	440	553	657
9	W_s	26	36	43	50	69	91
10	W_c	46	46	46	46	46	46
11	W_r	2	6	8	12	19	28
12	W_{rw}	100	98	98	97	96	95
13	Losses	174	186	195	205	230	260
14	W_{out}	24	136	187	234	322	397
15	Eff.	12	42	49	53	58	60

TABLE V. PERFORMANCE CALCULATIONS (60 HZ, 220 VOLTS)

Line No.	Description	Load Points 1	2	3	4	5	6
1	Slip	1.0	2.0	2.5	3.0	4.0	5.0
2	Z_2	227.1	113.7	91.0	75.9	57.1	45.8
3	R_o	45.1	50.6	49.4	47.2	42.1	37.4
4	jX_o	j78.2	j54.6	j46.0	j39.2	j30.2	j24.7
5	Z_o	90.27	74.45	67.50	61.37	51.80	44.80
6	P.F.	.500	.080	.732	.769	.813	.835
7	I_1	1.41	1.70	1.88	2.07	2.45	2.83
8	W_i	268	441	525	606	760	901
9	W_s	29	43	53	64	89	119
10	W_c	57	57	57	57	57	57
11	W_r	2	8	12	16	27	39
12	W_{rw}	135	133	132	131	130	128
13	Losses	222	240	253	268	303	343
14	W_{out}	46	203	272	339	457	558
15	Eff.	17	46	52	56	60	62

TABLE VI. PERFORMANCE CALCULATIONS (75 HZ, 272 VOLTS)

Line No.	Description	Load Points 1	2	3	4	5	6
1	Slip	1.0	2.0	2.5	3.0	4.0	5.0
2	Z_2	227.1	113.3	91.1	75.8	57.2	46.0
3	R_o	59.9	61.2	56.6	54.7	45.2	39.3
4	jX_o	j86.9	j53.2	j46.1	j38.5	j30.3	j25.3
5	Z_o	106.00	81.12	73.00	66.90	54.40	46.75
6	P.F.	.568	.734	.776	.803	.830	.840
7	I_1	1.50	1.91	2.15	2.39	2.89	3.36
8	W_i	397	660	786	906	1128	1330
9	W_s	33	56	69	82	124	167
10	W_c	77	77	77	77	77	77
11	W_r	4	13	18	25	40	58
12	W_{rw}	185	181	180	179	178	176
13	Losses	299	327	344	363	419	478
14	W_{out}	102	336	442	540	710	850
15	Eff.	25	51	56	60	63	64

$$R_o + jx_o = R + jx + R_1 + jx_1.$$

5. $Z_o = \sqrt{R_o^2 + jx_o^2}$.

6. Power factor $= \frac{R_o}{Z_o}$.

7. Per phase input current $I_1 = \frac{E_1}{Z_o}$.

8. Three phase input power $W_1 = nI_1^2 R_o$.

9. Three phase stator copper loss $W_s = nI_1^2 R_1$.

10. Core loss (eddy-current loss + hysteresis loss),

$$W_c = K_h \cdot f + K_e \cdot f^2.$$

From the equivalent circuit calculations, core loss at 60 hz was 57 watts. Assuming hysteresis loss is twice as great as eddy-current loss:

$$K_h = .6333,$$

$$K_e = .005278.$$

These constants in conjunction with line frequency are used to calculate loss.

11. Three phase rotor copper loss = air gap power · slip

$$W_r = S(W_i - W_s).$$

12. Rotational losses--W_{rw} are read directly from the graph on Figure 12, page 30.

13. Losses = $W_s + W_r + W_c + W_{rw}$.

14. Usable power out: $W_{out} = W_i$ - losses.

15. Per cent efficiency: $\text{Eff.} = 1 - \frac{(\text{losses})}{(W_i)} \cdot 100.$

Component values are taken from the equivalent circuit Figure 15, page 39. Experimental data obtained from actual machine performance is displayed in Tables VII, VIII and IX. The experimental and calculated values of slip vs output power can be compared on the graphs shown in Figures 16, 17 and 18. These figures indicate the equivalent circuits determined for three different frequencies which may be used to adequately predict induction motor performance. Analysis of the motor using other supply frequencies will be carried out in the same manner. A computer program to perform the calculations and print the results is shown in Appendix A. This program was used to calculate all predicted performance data.

TABLE VII. EXPERIMENTAL PERFORMANCE DATA (51 HZ, 186 VOLTS)

Point	Force (n)	Torque (n·m)	Slip (%)	Speed (rpm)	Current (a)	Power In (w)	Power Out (w)
1	0	0	.95	1513	1.20	205	0
2	3.78	.528	1.37	1509	1.30	240	84
3	4.45	.622	1.70	1504	1.35	265	98
4	6.67	.932	1.85	1501	1.50	320	147
5	8.90	1.243	2.60	1490	1.65	380	194
6	11.12	1.553	2.78	1487	1.90	430	242
7	13.34	1.864	3.10	1482	2.00	490	289
8	15.57	2.175	3.40	1478	2.15	550	337
9	17.80	2.490	4.10	1467	2.40	630	382
10	20.02	2.797	4.72	1458	2.60	700	427

TABLE VIII. EXPERIMENTAL PERFORMANCE DATA (60 HZ, 220 VOLTS)

Point	Force (n)	Torque (n·m)	Slip (%)	Speed (rpm)	Current (a)	Power In (w)	Power Out (w)
1	0	0	.83	1785	1.30	220	0
2	4.45	.622	1.33	1776	1.50	330	116
3	6.67	.932	1.83	1767	1.60	406	172
4	8.90	1.243	2.00	1764	1.80	480	230
5	11.12	1.553	2.50	1755	1.95	550	286
6	13.34	1.864	3.00	1746	2.15	630	341
7	15.57	2.175	3.33	1740	2.30	690	396
8	17.80	2.490	3.67	1734	2.50	740	452
9	20.02	2.797	4.16	1727	2.70	840	506
10	22.24	3.107	4.66	1716	2.90	930	559

TABLE IX. EXPERIMENTAL PERFORMANCE DATA (75 HZ, 272 VOLTS)

Point	Force (n)	Torque (n·m)	Slip (%)	Speed (rpm)	Current (a)	Power In (w)	Power Out (w)
1	0	0	.85	2231	1.30	320	0
2	2.89	.404	1.07	2226	1.50	424	94
3	4.45	.622	1.20	2220	1.55	450	145
4	6.67	.932	1.33	2217	1.55	470	216
5	8.90	1.243	1.74	2211	1.70	550	288
6	11.12	1.553	1.95	2206	1.85	620	359
7	13.34	1.864	2.10	2202	2.05	730	430
8	15.57	2.175	2.50	2191	2.20	820	499
9	20.02	2.797	3.47	2169	2.60	1000	635
10	24.46	3.417	4.53	2148	3.00	1270	769

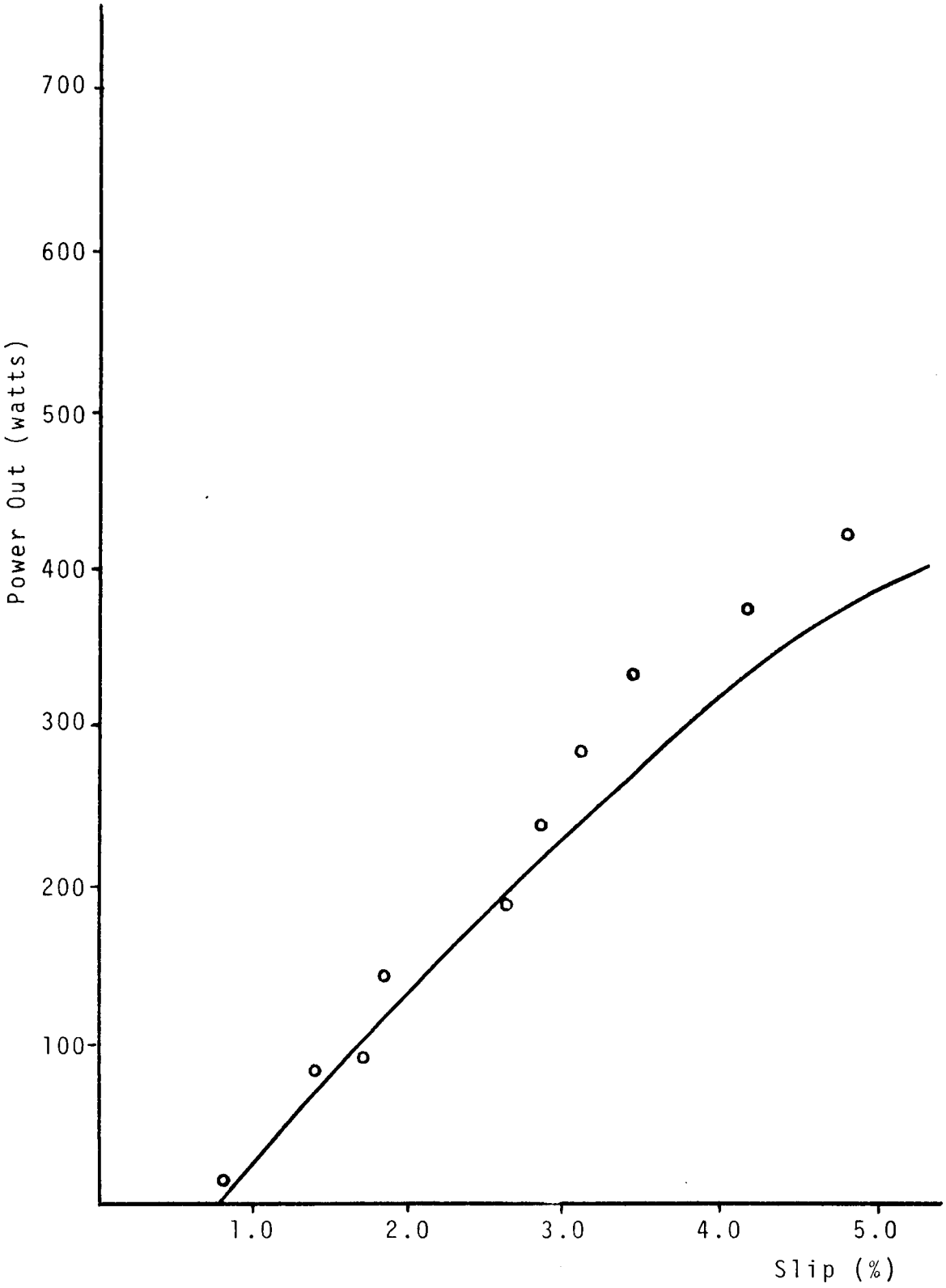

Figure 16. Power Out vs Slip (51 hz--186 v)

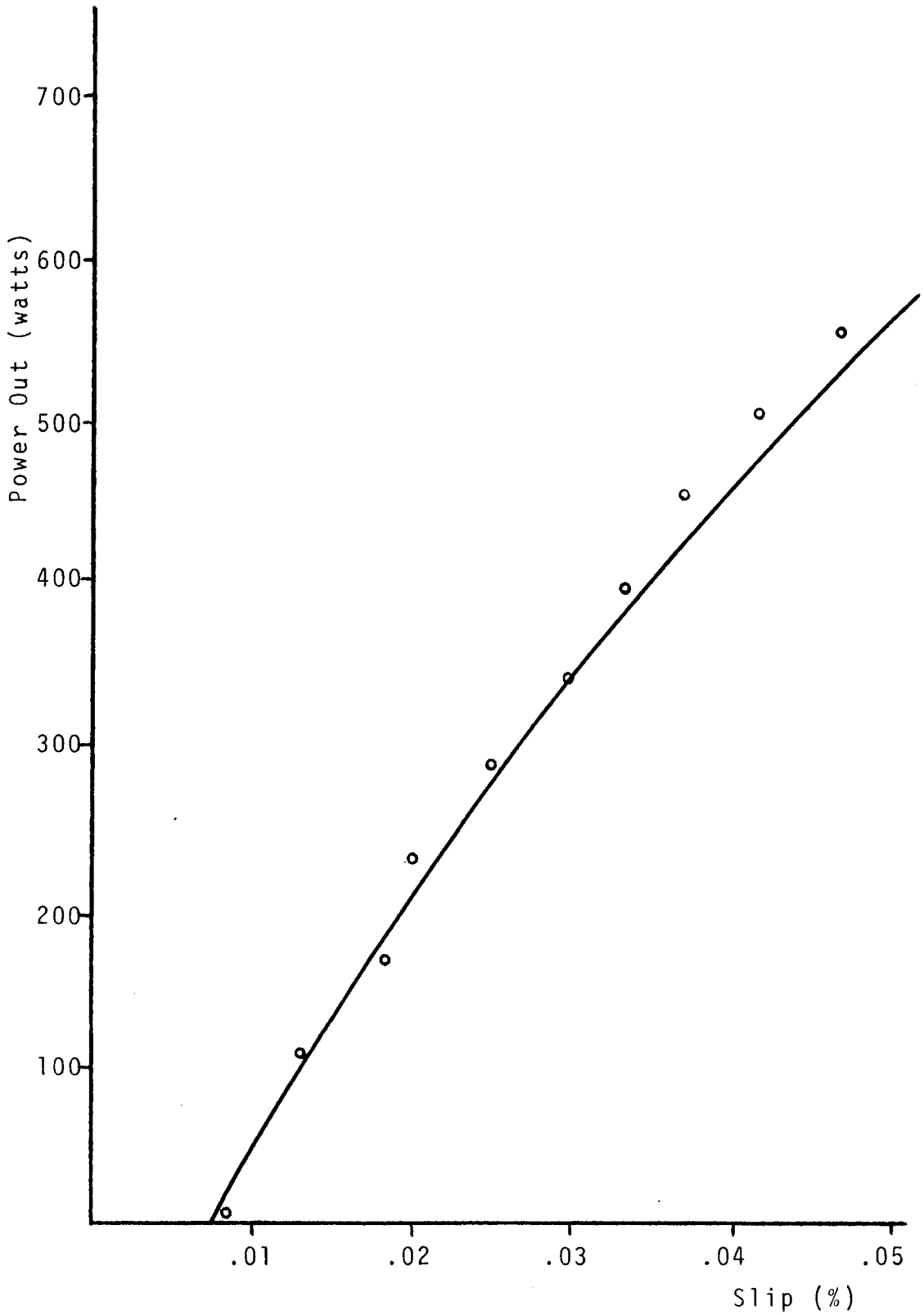

Figure 17. Power Out vs Slip (60 hz--220 v)

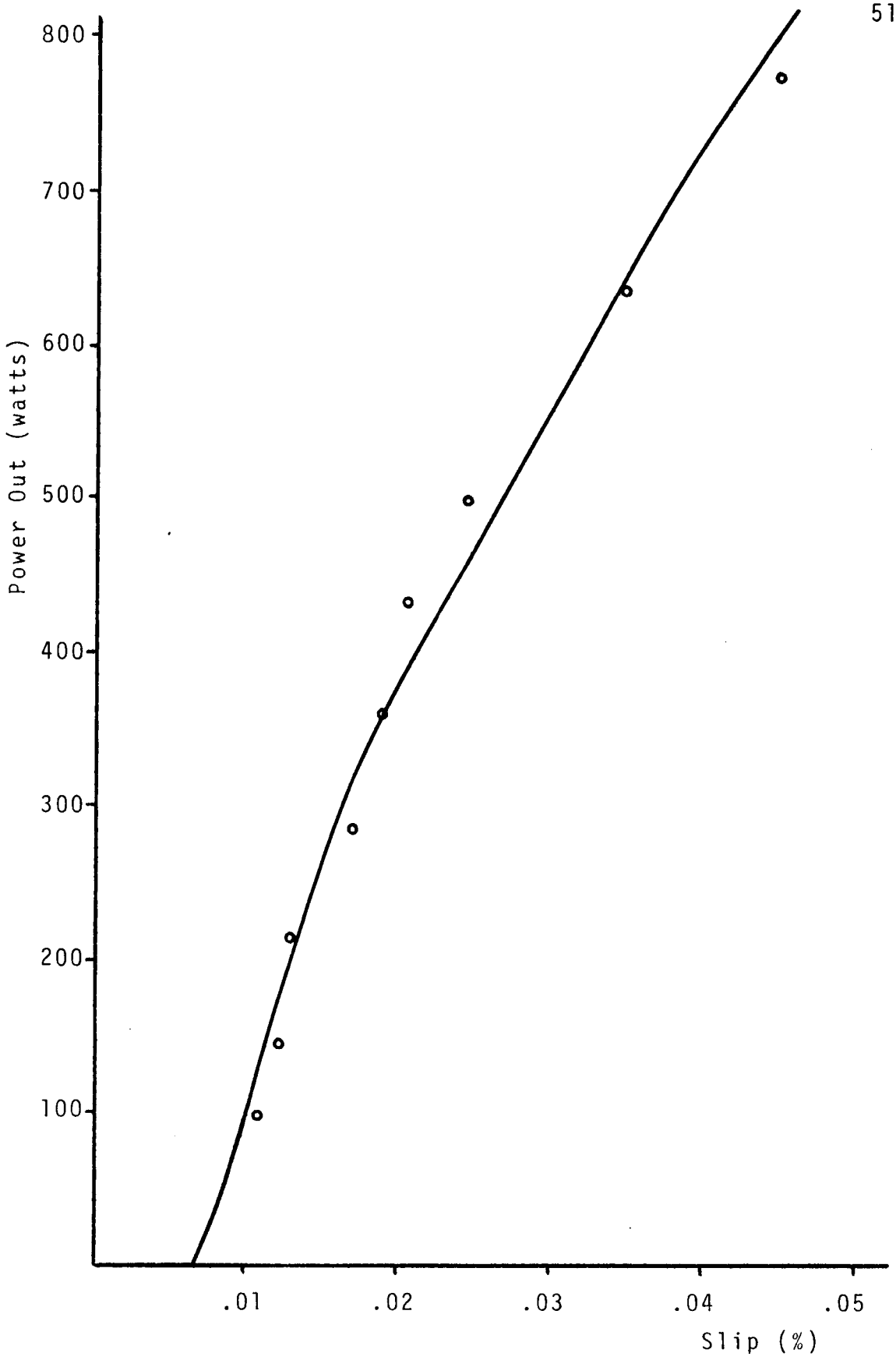

Figure 18. Power Out vs Slip (75 hz--272 v)

CHAPTER IV

MOTOR PERFORMANCE--NONSINUSOIDAL SOURCE

This chapter is an analysis of the performance of an induction motor when powered from a transistor-inverter. The inverter used was manufactured by PTI Controls, Model 1010-C. This system was supplied with an isolation transformer using single phase 60 cycle 220, 440 or 600 volts a-c for power. The three phase output voltage is a square wave capable of delivering 4.5 amps line current suitable for powering up to a 1 hp motor. Output frequency is adjustable from 6 to 60 hz through the setting of a potentiometer. Internal preset adjustments are high and low frequency stops, line current limiter and volts/hz constant.

This piece of equipment has been in operation in the textile industry for several years as part of a feedback network. The inverter powers two 1/2 hp induction motors which maintain proper tension on the cloth during processing. Choice of this system over a d-c motor system was a matter of reliability and lower initial investment. Servicing the motor controller is simplified with plug in modules.

I. FOURIER ANALYSIS

The first step in predicting motor performance is reducing the inverter output voltage into its sinusoidal components. The waveform is a square wave and therefore easily

broken down using Fourier Analysis.[7] The waveform is obviously periodic and conforms to Dirchlet conditions. The complete Fourier expansion for any such signal is:

$$f(\theta) = \frac{a_o}{2} + \sum_{n=1}^{\infty} (a_n \cos n\theta + b_n \sin n\theta),$$

$$a_o = \frac{1}{\pi} \int_{-\pi}^{\pi} f(\theta)\, d\theta$$

$$a_n = \frac{1}{\pi} \int_{-\pi}^{\pi} f(\theta) \cos n\theta\, d\theta \qquad (n = 0, 1, 2, 3\ldots),$$

$$b_n = \frac{1}{\pi} \int_{-\pi}^{\pi} f(\theta) \sin n\theta\, d\theta \qquad (n = 1, 2, 3\ldots).$$

A is the peak value of square wave.

D-C component:

$$a_o = \frac{1}{\pi} \int_{-\pi}^{\pi} f(\theta)\, d\theta,$$

$$a_o = \frac{1}{\pi} \left[\int_{-\pi}^{o} -A\, d\theta + \int_{o}^{\pi} A\, d\theta \right],$$

---

[7] David Cheng, Analysis of Linear Systems (Reading: Addison Wesley Publishing Company, Inc., 1961), pp. 121-135.

$$a_o = \frac{1}{\pi} [-A(o - (-\pi) + A(\pi - o)],$$

$$a_o = 0.$$

Cosine term coefficients:

$$a_n = \frac{1}{\pi} \int_{-\pi}^{\pi} f(\theta) \cos n\theta \, d\theta \qquad (n = 1, 2, 3...),$$

$$a_n = \frac{1}{\pi} [\int_{-\pi}^{o} -A \cos n\theta \, d\theta + \int_{o}^{\pi} A \cos n\theta \, d\theta],$$

$$a_n = \frac{1}{\pi} [- \frac{A}{n} (\sin o - \sin\pi(-n) + \frac{A}{n} (\sin\pi n - \sin o)],$$

$$a_n = 0 \text{ for all } n.$$

Sine term coefficients:

$$b_n = \frac{1}{\pi} \int_{-\pi}^{\pi} f(\theta) \sin n\theta \, d\theta \qquad (n = 1, 2, 3...),$$

$$b_n = \frac{1}{\pi} [\int_{-\pi}^{o} -A \sin n\theta \, d\theta + \int_{o}^{\pi} A \sin n\theta \, d\theta],$$

$$b_n = \frac{1}{\pi}\left[- \frac{A}{n} (-\cos o + \cos\pi(-n) + \frac{A}{n} (-\cos\pi n + \cos o) \right]$$

$$b_n = \frac{4A}{n} \qquad (n = 1, 3, 5...),$$

$$b_n = 0 \qquad (n = 2, 4, 6...).$$

Therefore the complete Fourier expansion:

$$f(\theta) = \frac{4A}{\pi}\left[\sin\theta + \frac{1}{3}\sin 3\theta + \frac{1}{5}\sin 5\theta... \right].$$

II. PERFORMANCE CALCULATIONS

The harmonic components of the input voltage were each applied to a particular equivalent circuit. The frequency dependent values for these circuits were scaled for each harmonic. The fundamental frequency performance was calculated exactly as in the previous chapter. A computer program was used to calculate all parameters for six values of slip. The harmonic frequencies used the same method for only one value of slip. This slip was determined as follows:[8]

---

[8]Eugene A. Klingshirn, Polyphase Induction Motor Performance and Losses on Nonsinusoidal Voltage Sources (New York: IEEE Trans. Paper No. 31 TP67-472, 1967), pp. 526.

$$s = \frac{n \pm 1}{n} \quad \text{where}$$

n = harmonic,

+ = backward revolving field,

- = forward revolving field.

Harmonic	Sign
3	+
5	-
7	+
9	-
11	+

Core loss for each frequency was calculated. The constants for the magnetic material were the same as used in Chapter III. The individual core losses were then multiplied by a fraction to account for the reduced magnetic saturation. The formula used is:

$$W_c = \left(\frac{V_{2n}}{V_{2x}}\right)^2 (k_h f_n + k_e f_n^2)$$

$k_h = .6333,$

$k_e = .005278,$

V_{2n} = harmonic voltage applied to magnetizing circuit.

f_n = harmonic frequency,

$$V_{2x} = \frac{119 \cdot f_n}{60}.$$

V_{2x} is the voltage applied to the rotor which would give the same magnetic saturation at the harmonic frequency as is given by the normal V_2 voltage at 60 cycles.

The summation of the core losses for the three data sets are:

20 hz--27 watts,

40 hz--51 watts,

60 hz--65 watts.

Lower frequency has less core loss because eddy-current loss is proportional to the frequency squared. The reduced operating voltage at the lower frequencies causes a correspondingly lower core loss. These calculations were done for the fundamental, 3rd, 5th, 7th, 9th and 11 harmonics.

Figures summarizing the performance calculations for 20, 40 and 60 hz operation are given in Tables X, XI and XII. Actual performance data obtained by experimental methods are shown on Tables XIII, XIV and XV. The power-in vs slip and power-out vs slip graphs compare experimental and calculated values. These graphs are shown in Figures 19 through 24.

TABLE X

RESULTS OF PERFORMANCE CALCULATIONS (20 HZ, 115 VOLTS P-P)

Fundamental Frequency 51.7 volts rms						
Slip	1.0	2.0	2.5	3.0	4.0	5.0
Current	1.5	1.53	1.55	1.58	1.66	1.74
Power In	83	110	124	138	164	189
Power Out	-1	25	37	48	70	89

Harmonic Frequencies				
Number	RMS Volts	Current	Power In	Power Out
3	17.3	1.3	36.6	-2.6
5	10.4	.5	5.6	.39
7	7.4	.26	1.6	-.04
9	5.8	.16	.8	.02
11	4.7	.11	.4	-.05

Composite Response						
Slip	1.0	2.0	2.5	3.0	4.0	5.0
Power In	128	155	169	183	209	234
Power Out	-3	23	35	46	68	87

TABLE XI

RESULTS OF PERFORMANCE CALCULATIONS (40 HZ, 210 VOLTS P-P)

Fundamental Frequency 94.5 volts rms						
Slip	1.0	2.0	2.5	3.0	4.0	5.0
Current	1.45	1.61	1.71	1.83	2.07	2.30
Power In	177	274	321	367	454	539
Power Out	27	114	154	192	261	322

Harmonic Frequencies				
Number	RMS Volts	Current	Power In	Power Out
3	31.5	1.30	39.3	-2.85
5	18.9	.47	5.8	.41
7	13.5	.25	1.8	-.05
9	10.5	.15	.8	.03
11	8.6	.10	.4	-.01

Composite Response						
Slip	1.0	2.0	2.5	3.0	4.0	5.0
Power In	225	322	369	415	502	587
Power Out	25	112	152	190	259	320

TABLE XII

RESULTS OF PERFORMANCE CALCULATIONS (60 HZ, 270 VOLTS P-P)

Fundamental Frequency 122 volts rms						
Slip	1.0	2.0	2.5	3.0	4.0	5.0
Current	1.35	1.63	1.80	1.98	2.35	2.70
Power In	257	411	493	567	707	837
Power Out	37	180	245	306	414	507

Harmonic Frequencies				
Number	RMS Volts	Current	Power In	Power Out
3	40.5	1.14	32.9	-2.50
5	24.3	.42	5.2	.38
7	12.4	.21	1.8	-.06
9	13.5	.13	.8	.10
11	11.0	.09	.4	.00

Composite Response						
Slip	1.0	2.0	2.5	3.0	4.0	5.0
Power In	298	452	534	608	748	878
Power Out	35	178	234	304	412	505

TABLE XIII. NONSINUSOIDAL MEASURED PERFORMANCE DATA (20 HZ, 115 VOLTS P-P)

Point	Motor Data				Inverter Data	
	Slip (%)	Power Out (watts)	Current (amps)	Power In (watts)	Current (amps)	Power In (watts)
1	2.0	0	1.70	110	2.40	200
2	2.5	25	1.70	149	3.00	230
3	3.0	34	1.75	155	3.20	240
4	3.4	52	1.80	175	3.60	270
5	4.0	71	1.85	200	4.00	300
6	4.7	85	1.95	220	4.30	340
7	5.5	107	2.00	245	4.85	360
8	6.3	120	2.20	260	5.20	405
9	8.0	140	2.30	310	5.75	430

TABLE XIV. NONSINUSOIDAL MEASURED PERFORMANCE DATA (40 HZ, 210 VOLTS P-P)

Point	Motor Data				Inverter Data	
	Slip (%)	Power Out (watts)	Current (amps)	Power In (watts)	Current (amps)	Power In (watts)
1	1.00	0	1.45	170	2.2	260
2	1.50	69	1.65	265	3.1	380
3	1.80	75	1.70	300	3.5	410
4	2.50	145	1.85	370	4.0	480
5	2.90	205	2.00	430	4.5	535
6	3.50	219	2.10	465	4.8	590
7	4.10	250	2.25	510	5.1	620
8	4.50	291	2.40	560	5.6	700
9	5.15	325	2.50	630	6.1	765
10	6.00	360	2.70	670	6.5	820

TABLE XV. NONSINUSOIDAL MEASURED PERFORMANCE DATA (60 HZ, 270 VOLTS P-P)

Point	Motor Data				Inverter Data	
	Slip (%)	Power Out (watts)	Current (amps)	Power In (watts)	Current (amps)	Power In (watts)
1	0.80	0	1.35	285	2.4	370
2	1.50	104	1.55	365	3.9	480
3	1.90	195	1.70	460	4.2	550
4	2.33	218	1.80	495	4.9	600
5	3.00	295	1.95	580	5.2	690
6	3.33	329	2.15	645	5.3	780
7	3.60	410	2.35	755	5.7	890
8	4.30	437	2.50	795	6.0	960
9	5.10	500	2.80	950	7.2	1100
10	6.33	538	3.10	1000	7.7	1200

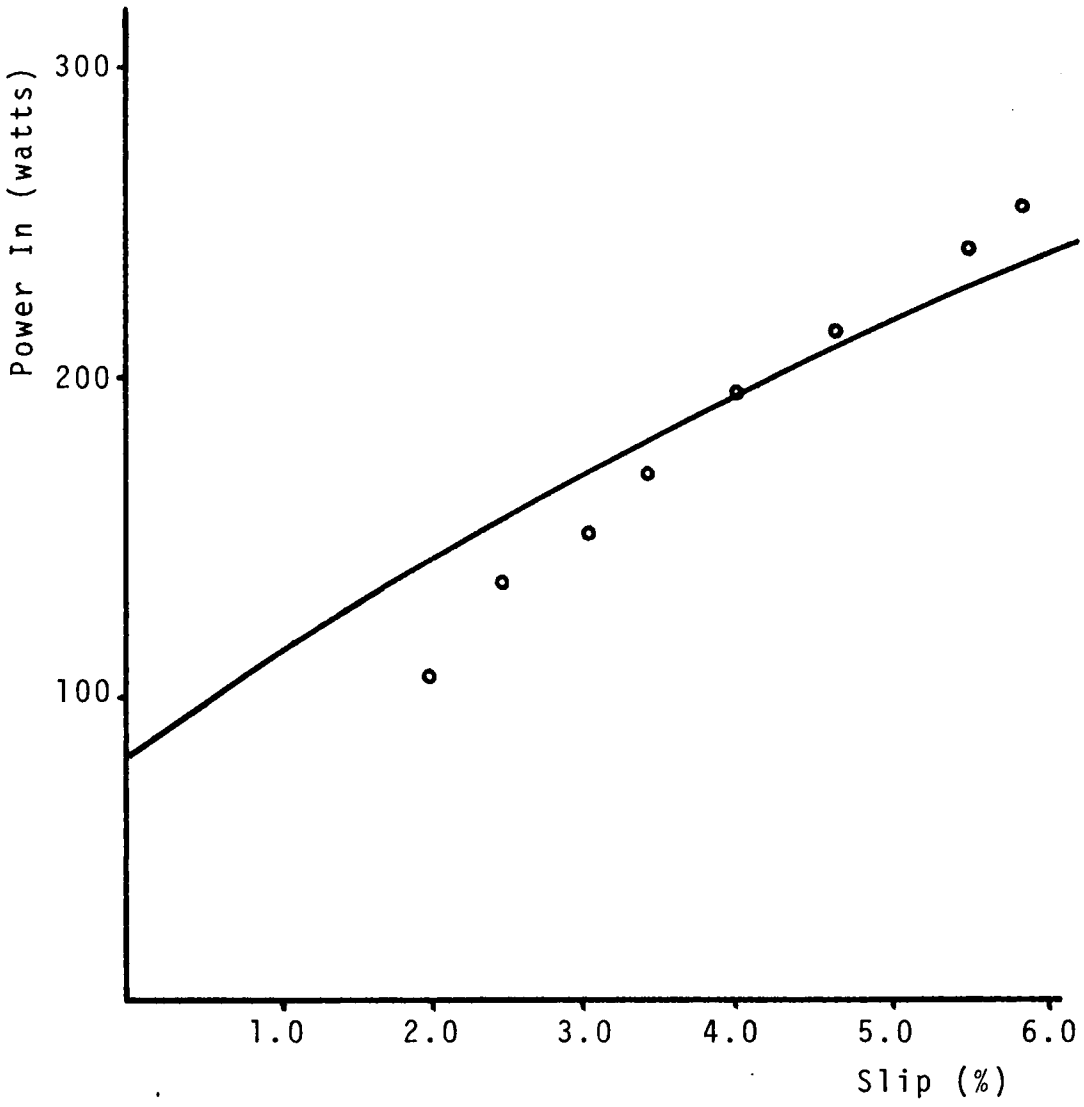

Figure 19. Motor Power In vs Slip (20 hz operation)

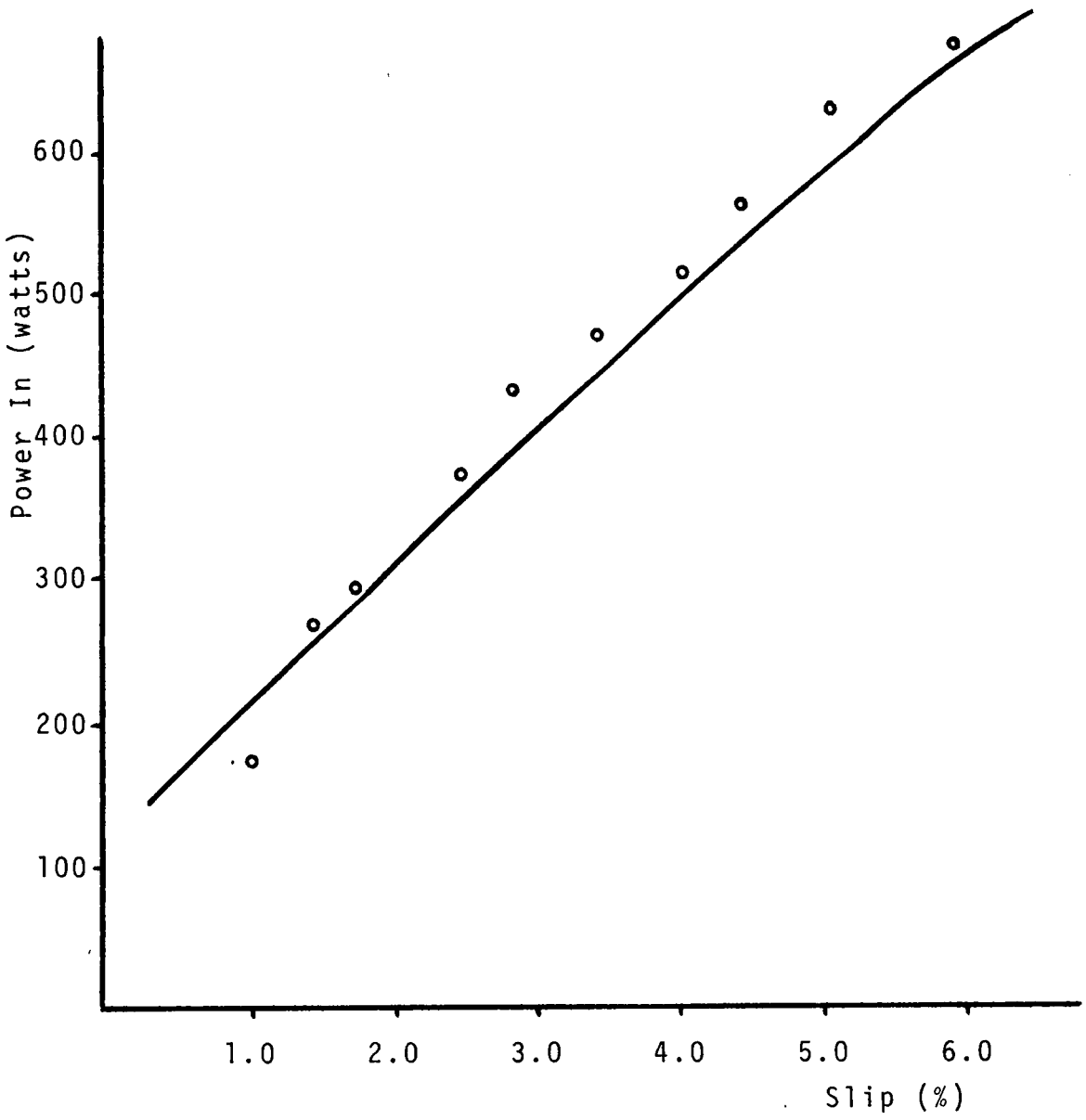

Figure 20. Motor Power In vs Slip (40 hz operation)

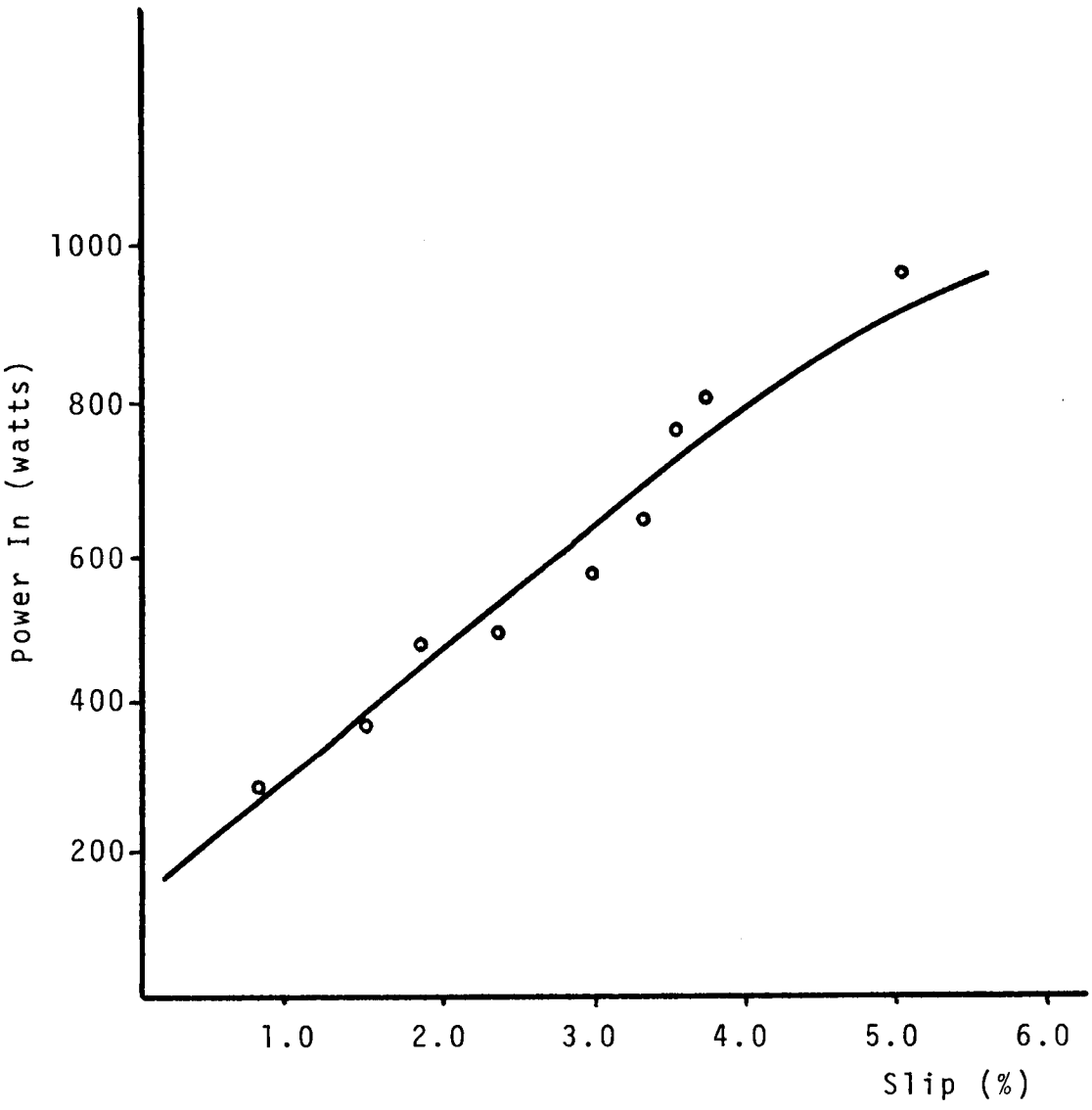

Figure 21. Motor Power In vs Slip (60 hz operation)

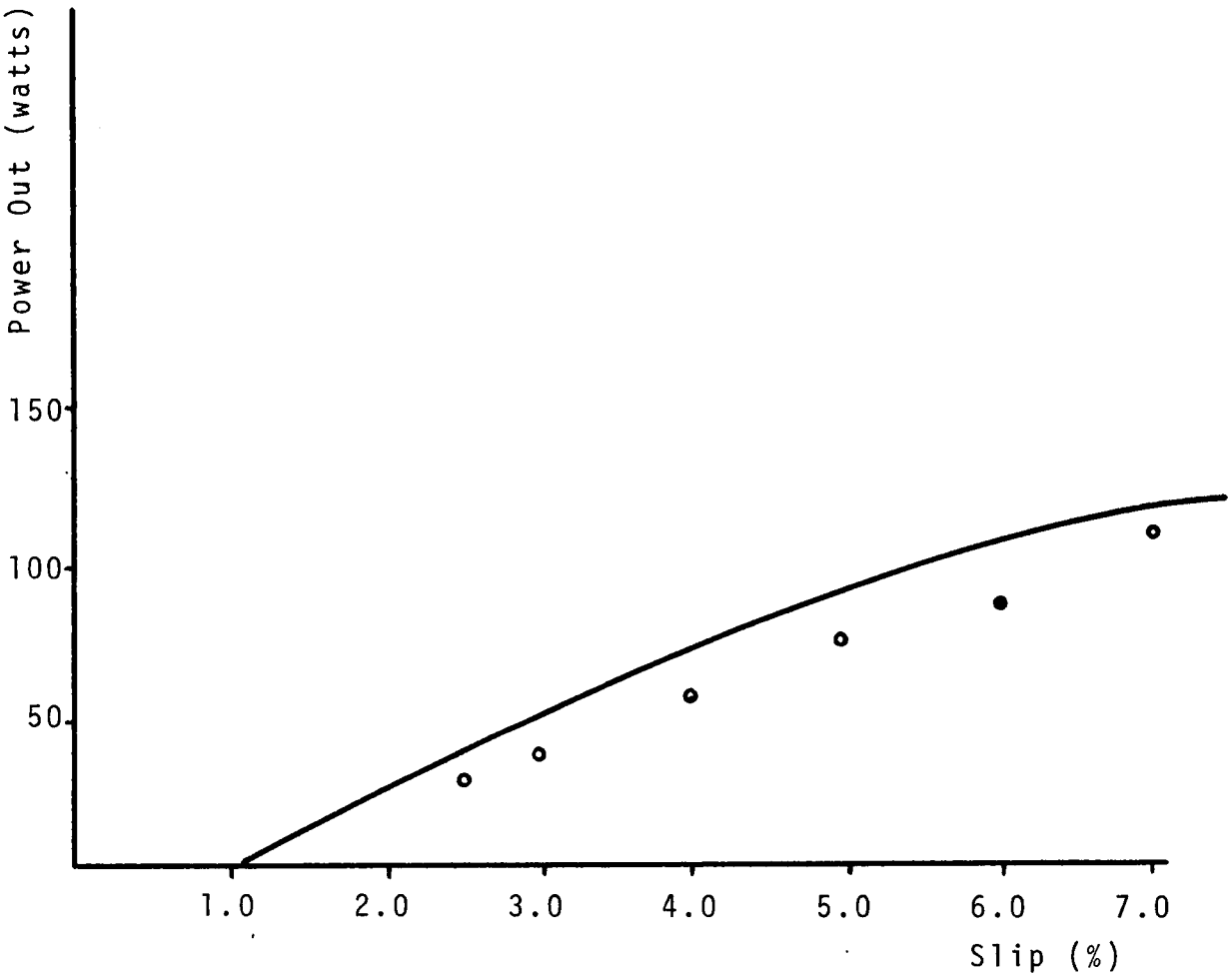

Figure 22. Power Out vs Slip (20 hz operation)

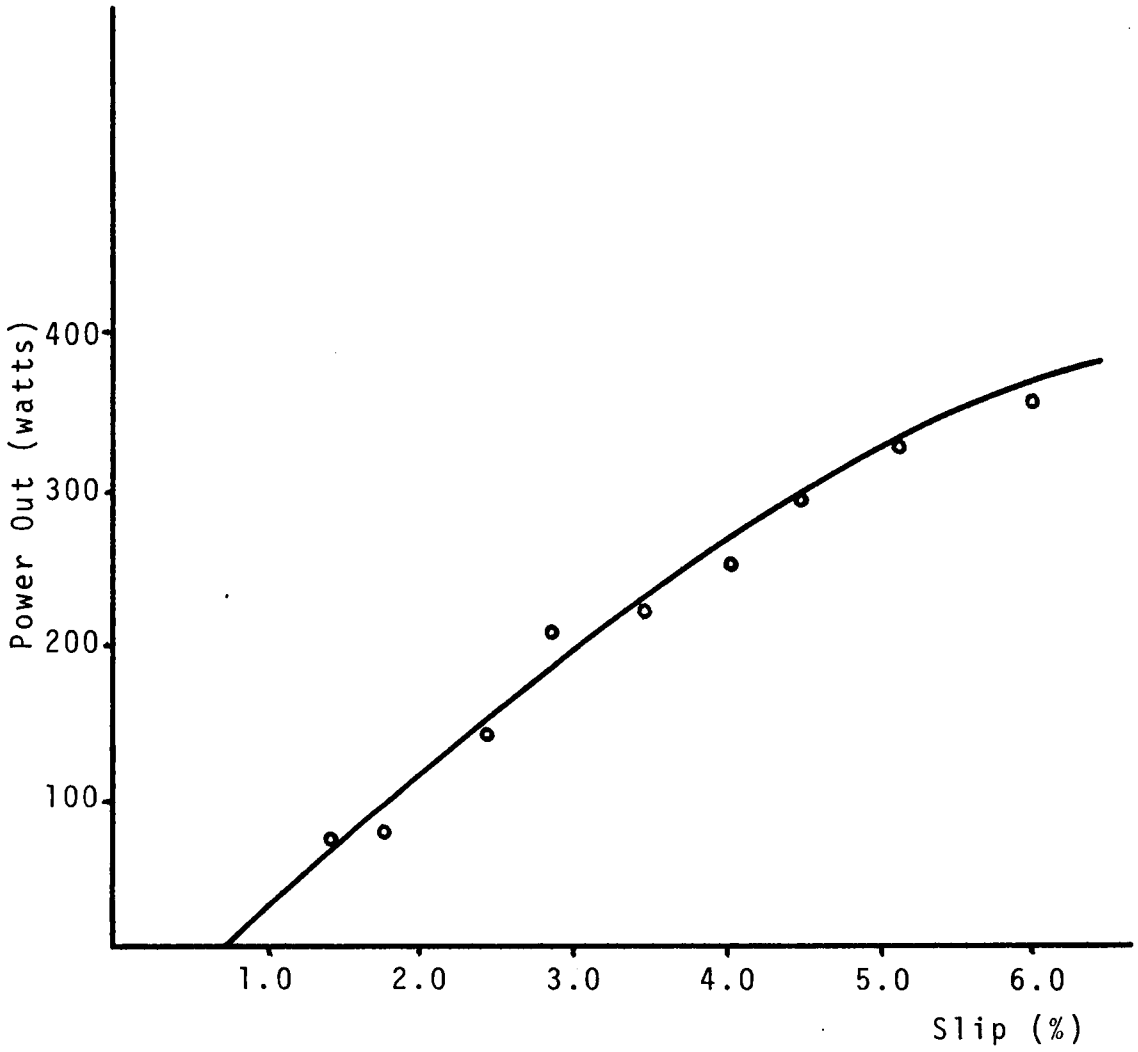

Figure 23. Power Out vs Slip (40 hz operation)

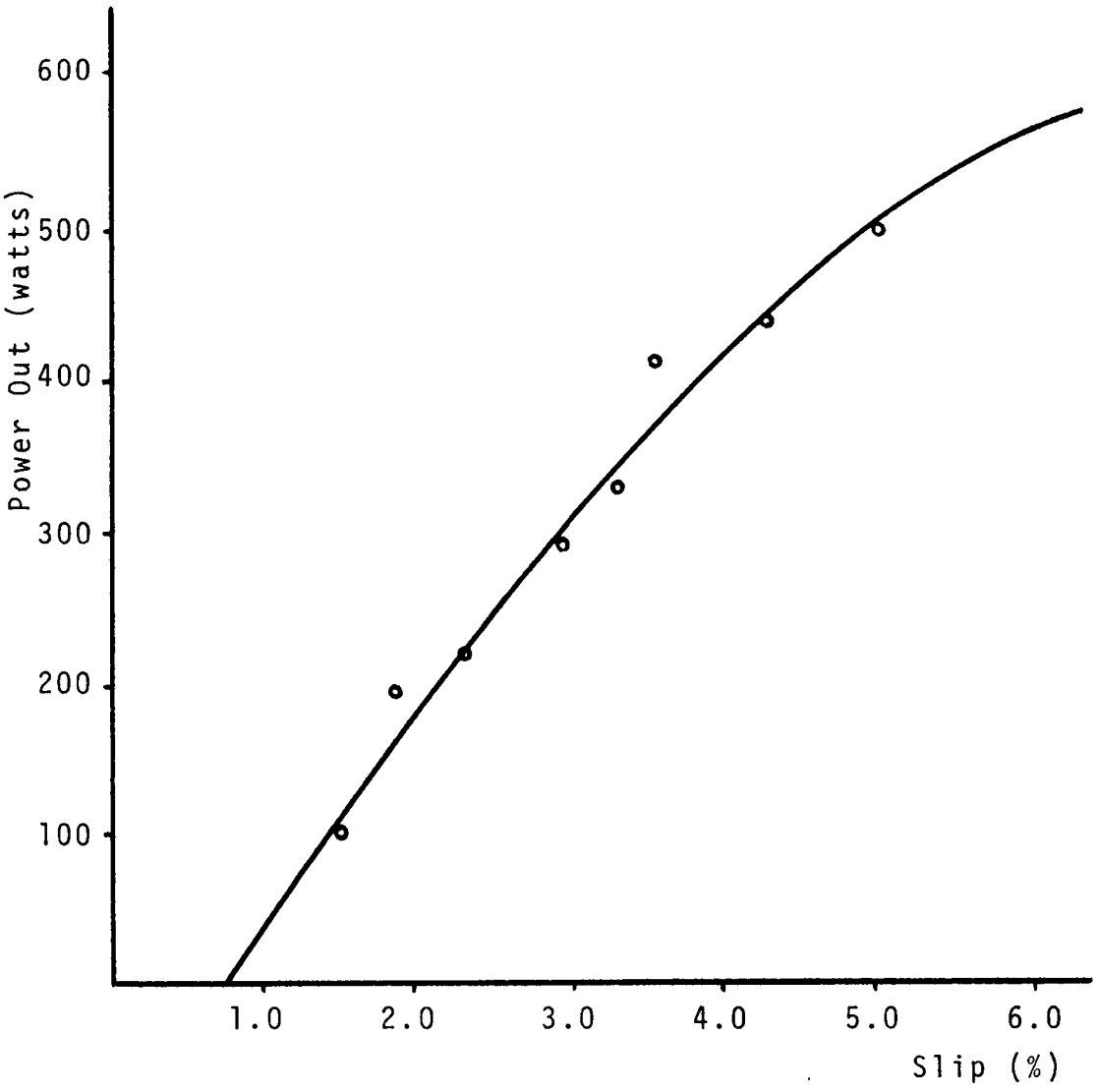

Figure 24. Power Out vs Slip (60 hz operation)

III. WAVEFORM ANALYSIS

Figures 25 through 33 show operating voltage and current waveforms to the motor. Complete descriptions of these oscilloscope photographs are adjoining the pictures. The line-to-neutral and line-to-line voltage waveforms are, as was expected, simple rectangular waves. The line current waveforms are complex waveforms composed of an infinite number of harmonics of various phases and amplitudes.

To synthesize these waveforms would lend considerable credibility to the motor analysis program. These current harmonics are a result of the voltage harmonics present in the input waveform. The first step would be to determine the phases of the input voltages. Returning to Fourier analysis, the complete series could have been expressed as:

$$f(t) = \frac{a_0}{2} + \sum_{n=1}^{\infty} c_n \cos(nwt - \psi_n),$$

$$c_n = \sqrt{a^2_n + b_n^2}$$

$$\psi_n = \tan^{-1} \left(\frac{b_n}{a_n}\right).^9$$

---

[9] Cheng, op. cit., p. 124.

Figure 25. 60 Cycle Line-To-Neutral Voltage
(Vertical--50 v/div, Horizontal--5 ms/div)

Figure 26. 60 Cycle Line-To-Line Voltage
(Vertical--Uncalibrated, Horizontal--2 ms/div)

Figure 27. 60 Cycle Line Current
(Vertical--Uncalibrated, Horizontal--5 ms/div)

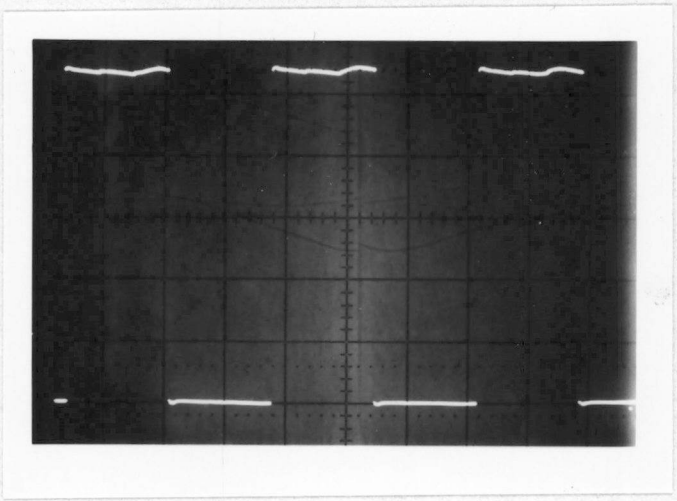

Figure 25.

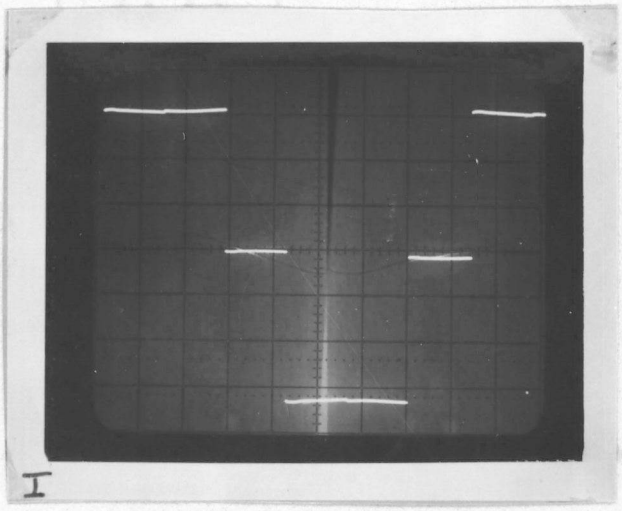

Figure 26.

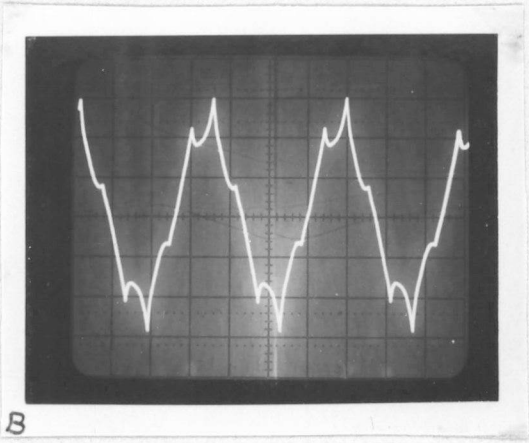

Figure 27.

Figure 28. 40 Cycle Line-To-Neutral Voltage
(Vertical--50 v/div, Horizontal--5 ms/div)

Figure 29. 40 Cycle Line-To-Line Voltage
(Vertical--Uncalibrated, Horizontal--5 ms/div)

Figure 30. 40 Cycle Line Current
(Vertical--Uncalibrated, Horizontal--5 ms/div)

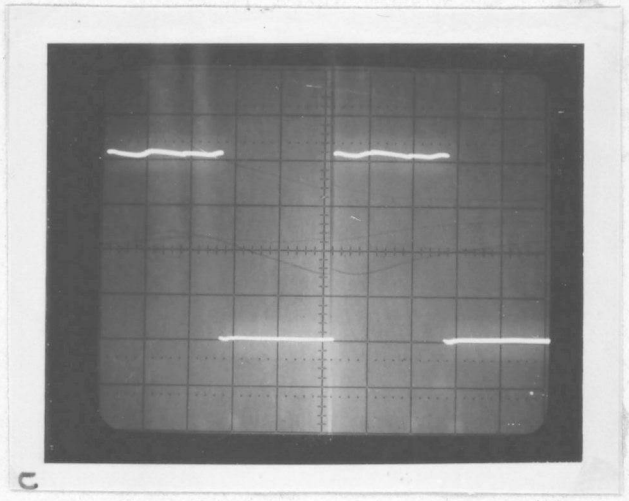

Figure 28.

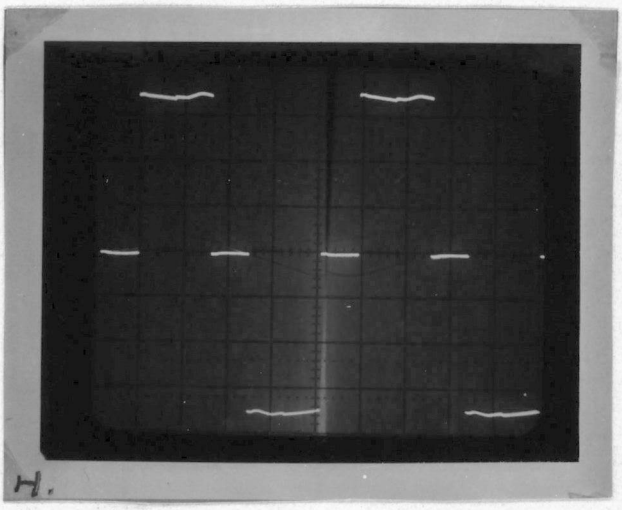

Figure 29.

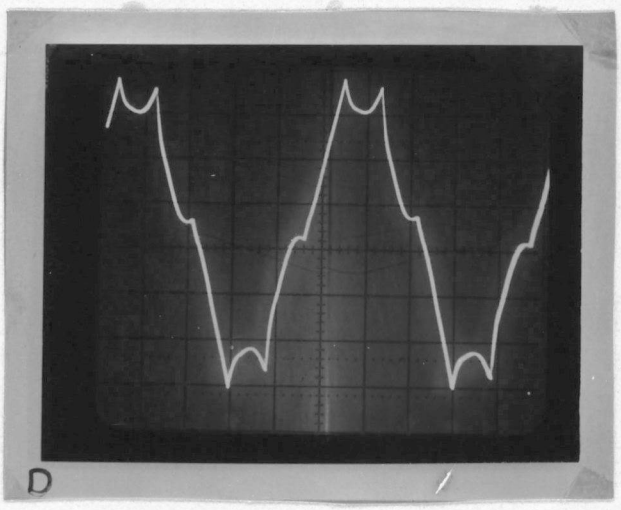

Figure 30.

Figure 31. 20 Cycle Line-To-Neutral Voltage
(Vertical--20 v/div, Horizontal--10 ms/div)

Figure 32. 20 Cycle Line-To-Line Voltage
(Vertical--Uncalibrated, Horizontal--10 ms/div)

Figure 33. 20 Cycle Line Current
(Vertical--Uncalibrated, Horizontal--10 ms/div)

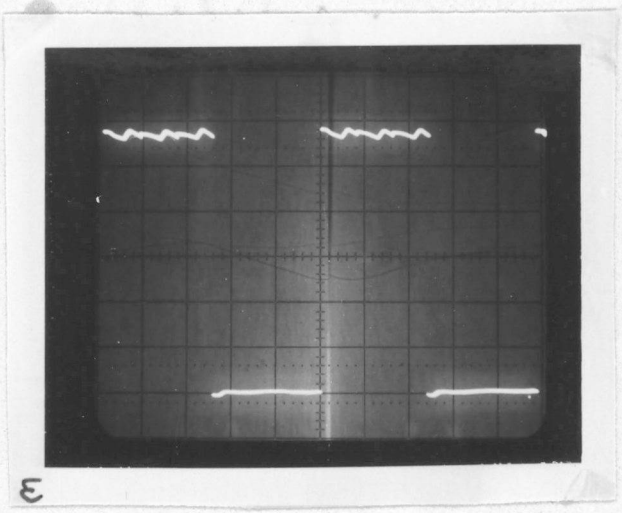

Figure 31.

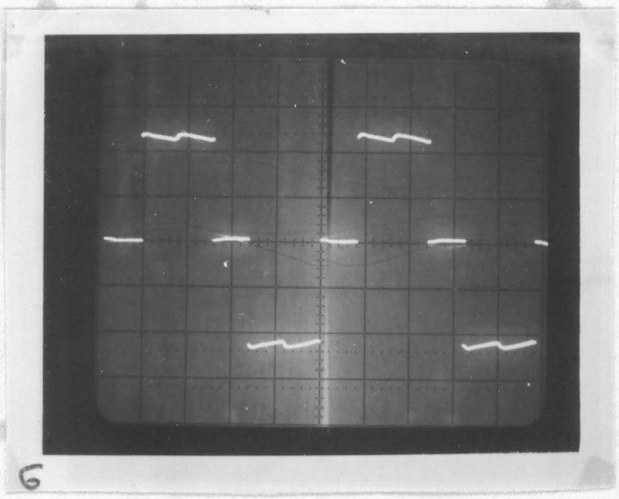

Figure 32.

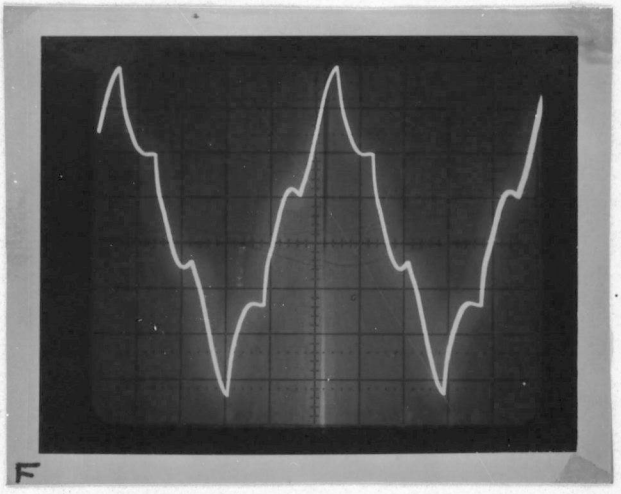

Figure 33.

Using this relationship, the phases of the voltage harmonics can be calculated. The coefficients were earlier determined to be:

$$a_n = 0,$$

$$b_n = \frac{4}{\pi \cdot n}$$

$$\Psi_n = \tan^{-1} \left(\frac{4}{\pi \cdot n}\right)/0,$$

$$\Psi_n = \tan^{-1} (\infty) \qquad \text{for all } n.$$

All voltage harmonics, therefore, are phased alike. The current harmonics and their phases were calculated using the motor performance computer program. To synthesize the current waveform, it is only necessary to combine harmonics. A program is given in Appendix A to perform the operation.

Tracings of the computer printouts for three synthesized waveforms are shown in Figures 34, 35 and 36. These tracings compare favorably to the photographs taken of the actual current waveforms. The absence of sharp transitions in the computer graph is because of lack of high frequency components.



Figure 34. Synthesized Current Waveform--60 hz

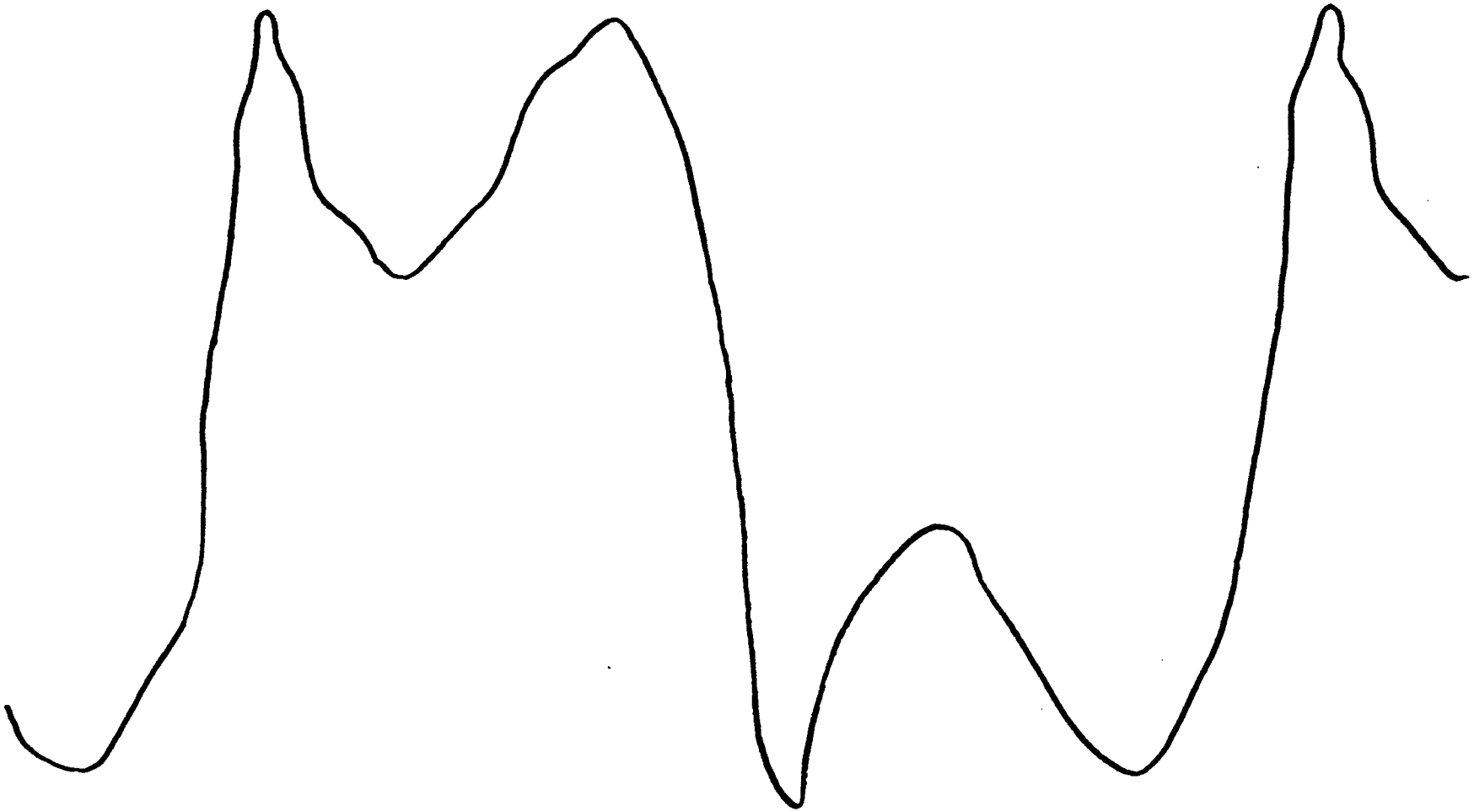

Figure 35. Synthesized Current Waveform--40 hz

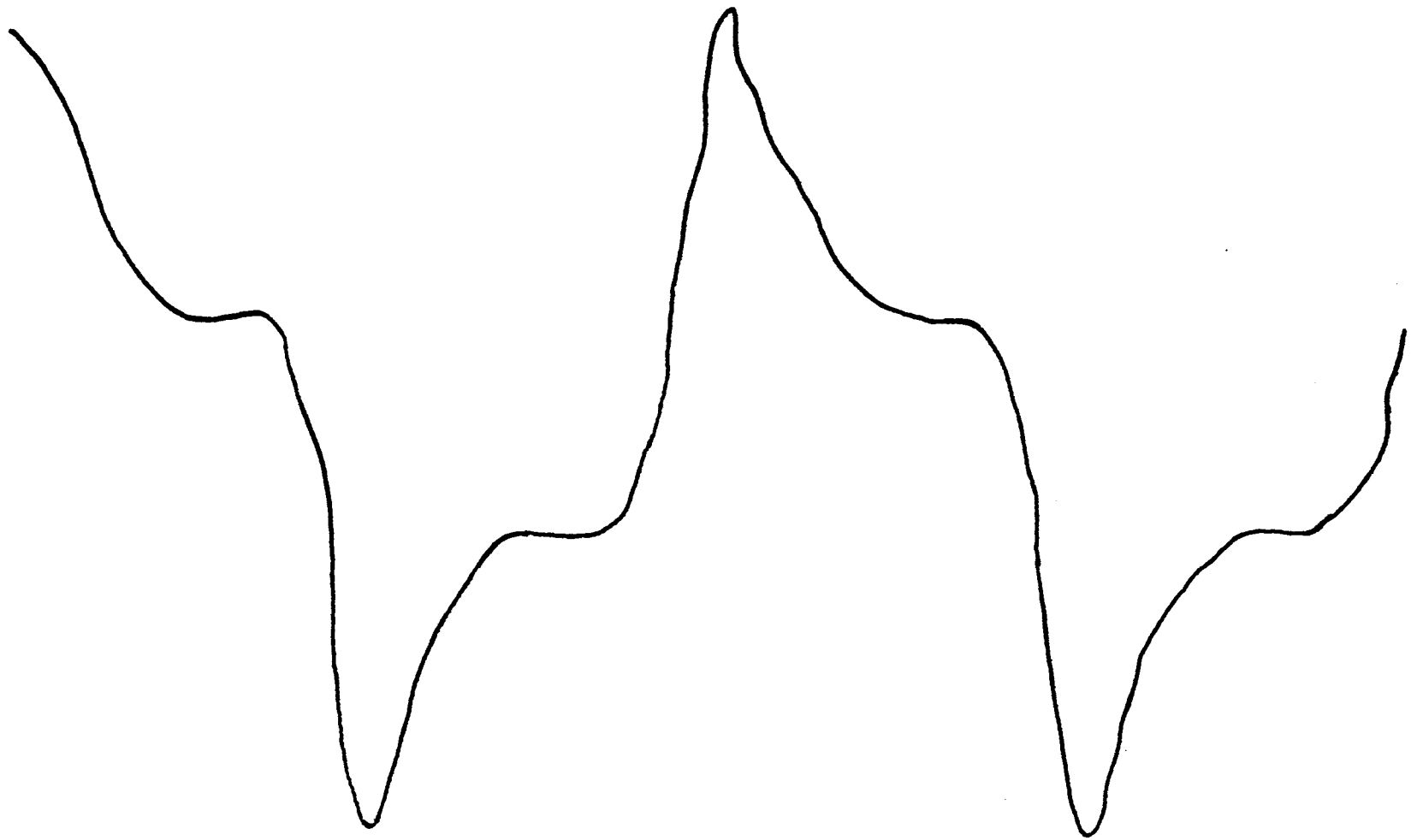

Figure 36. Synthesized Current Waveform--20 hz

CHAPTER V

SYSTEM PERFORMANCE CONSIDERATIONS

I. MOTOR PERFORMANCE

Experimental and Calculated Data

The intent of this work was to study the effects of a solid state inverter on the performance of a three phase induction motor. A necessary part of this goal was the development of a method of analysis to predict this performance. Comparison of experimental and calculated performance parameters indicates the technique is a viable one. In Chapter IV both power-in and power-out were calculated for three operating frequencies and compared to experimental values. In the analysis of a motor powered by a nonsinusoidal voltage source the steps are:

1. Obtain rotational loss profile.
2. Develop the motor equivalent circuit.
3. Determine core loss for the standard operating frequency. The constants for eddy-current and hysteresis are calculated.
4. Resolve applied voltage waveform into its fundamental components. Each component is applied to an equivalent circuit. The equivalent circuits all have the frequency dependent values properly scaled to the applied harmonic. The individual circuit

responses are summed to provide the composite responses.

These steps are to be considered a brief summary of the method of analysis. For a more detailed summary refer to Chapters III and IV.

From a motor power-out standpoint, the summation of the harmonics produces a negligible power-out. All power associated with the harmonics, therefore, is treated as a loss. Total harmonic losses for the three frequencies evaluated were:

20 hz--45 watts,

40 hz--46 watts,

60 hz--41 watts.

These losses occur independent of load. For the 60 cycle case, the decrease in efficiency of the input power ranges from 7-20%. A computer program was written to perform the tedious calculations for this analysis. The program was used to calculate operating parameters for both sinusoidal and nonsinusoidal operation. In the nonsinusoidal case power-in, power-out and losses of the various harmonics were added in a separate operation to form the composite response. This technique results in excellent correlation over the entire operating range.

Efficiency Improvements Due to Reduction in Harmonic Content

The output voltage waveform of the inverter used in this analysis was a rectangular wave with 180 degree conduction.

The high harmonic content of this waveform presents a worst case example. The rectangular waveform has odd harmonics present in decreasing amplitudes out to infinity. These harmonics present the motor with unusable energy which must be dissipated as heat. Reductions in the harmonic content of the applied voltage will improve motor performance accordingly.

To quickly evaluate the harmonic content of various waveforms, a computer program was written. The coefficient formulae are taken from page 53, and T is the period of the waveform--f(t) being evaluated. Substituting into the equation for a_o, a_n and b_n:

$$\theta = wt = 2\pi t,$$

$$a_o = \frac{2}{T} \int_{-T/2}^{T/2} f(t)\, dt,$$

$$a_n = \frac{2}{T} \int_{-T/2}^{T/2} f(t) \cos n\, wt\, dt,$$

$$b_n = \frac{2}{T} \int_{-T/2}^{T/2} f(t) \sin n\, wt\, dt.$$

The equation for the Fourier coefficients are suitable for solution using a digital computer if they are in the

form of a Riemann integral.[10] In this format, the area under the integral is partitioned into a finite number of intervals. Each interval is solved and the results of all intervals are added for the final results. The coefficient formulae expressed in a summation format are:

$$a_o = \sum_{k=1}^{m} f\left(k \cdot \frac{1}{m}\right) \cdot \frac{1}{m}$$

$$a_n = 2 \sum_{k=1}^{m} \frac{f\left(k \cdot \frac{1}{m}\right)}{m} \cos\left\{n \cdot 2\pi\left(k \cdot \frac{1}{m}\right)\right\}$$

$$b_n = 2 \sum_{k=1}^{m} \frac{f\left(k \cdot \frac{1}{m}\right)}{m} \sin\left\{n \cdot 2\pi\left(k \cdot \frac{1}{m}\right)\right\}$$

Each harmonic frequency--n is solved for each portion--m. The results are added. The greater the number of partitions the better the accuracy. A computer program to perform these operations is shown in Appendix A.

The results of this analysis for two waveforms are shown in Figures 37 and 38. The pulse waveform and multi-stepped waveform represent two different approaches of harmonic reduction. Either of these waveforms would result

---

[10] Watson Fulks, Advanced Calculus (New York: John Wiley and Sons, Inc., 1969), pp. 99-150.

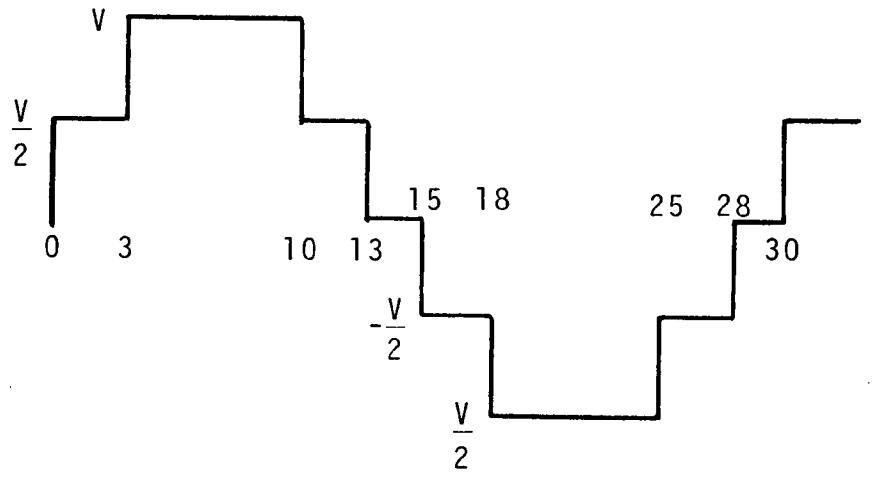

$$f(t) = .219 \cdot V \cdot \sin t + 1.03 \cdot V \cdot \cos t$$
$$+ .094 \cdot V \cdot \sin 9t$$
$$+ .07 \cdot V \cdot \sin 11t + .06 \cdot V \cdot \cos 11t$$
$$+ .02 \cdot V \cdot \sin 13t + .05 \cdot V \cdot \cos 13t$$
$$+ .01 \cdot V \cdot \sin 17t + .03 \cdot V \cdot \cos 17t$$

Figure 37. Rectangular Wave and Harmonic Content

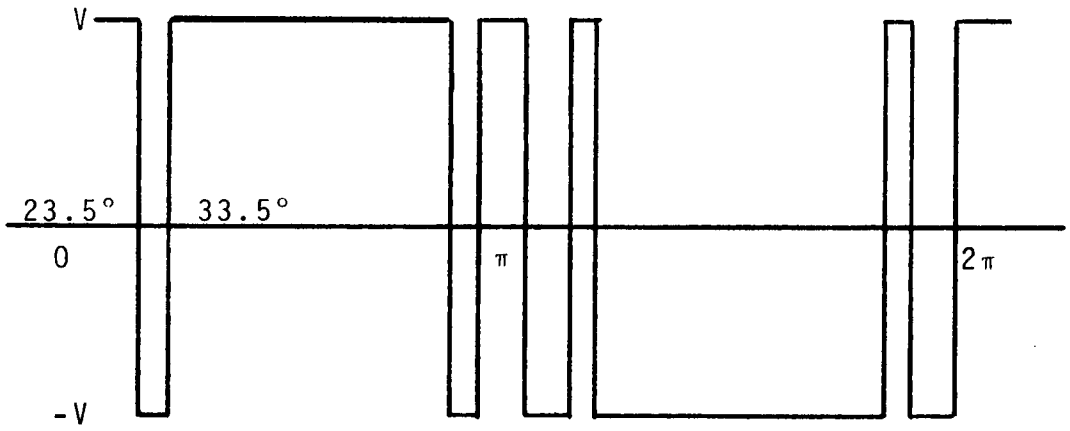

$$f(t) = 1.08 \cdot V \cdot \cos t$$
$$+ .3 \cdot V \cdot \cos 7t$$
$$+ .5 \cdot V \cdot \cos 9t$$
$$+ .37 \cdot V \cdot \cos 11t$$
$$+ .2 \cdot V \cdot \cos 15t$$
$$+ .17 \cdot V \cdot \cos 17t$$

Figure 38. Pulsed Wave and Harmonic Content

in a considerable improvment in motor efficiency. Increased complexity of the inverter section and possible higher inverter losses would have to be considered when using these waveforms.

II. INVERTER PERFORMANCE

Table XVI is a collection of five data points from each of the three frequencies tested. As stated in the table, both efficiency and power factor increase rapidly as frequency increases. Power factor at 20 hz is .35; this low value would be unacceptable in any large scale use of power and would require power factor correction measures. Worst case efficiency is 55% occurring at minimum load 20 hz operation, while best efficiency is 86% occurring at maximum load 60 hz operation. The lower efficiency at 20 hz can be attributed to lesser amounts of power being handled. Inverter losses seem to stay at a relatively constant 100 watts. This power is for generation of logic and gating signals. The most pertinent observation at this point is that inverter losses exceed motor harmonic losses by a factor of two.

TABLE XVI. INVERTER PERFORMANCE DATA

Current In (a)	Power In (w)	P.F.	Power Out (w)	Eff. (%)	Loss (w)
		Frequency--20 hz			
2.4	200	.38	110	55	90
3.2	240	.34	155	64	85
4.0	300	.34	200	66	100
4.8	360	.33	245	68	115
5.8	430	.34	310	72	120
		Frequency--40 hz			
2.2	260	.54	170	65	90
4.0	480	.54	370	77	110
4.8	590	.56	464	79	125
5.6	700	.57	560	80	140
6.5	820	.57	670	82	150
		Frequency--60 hz			
2.4	370	.70	285	77	85
4.2	550	.60	460	84	90
5.2	690	.60	580	84	110
5.7	890	.78	755	85	135
7.2	1100	.70	950	86	160

CHAPTER VI

CONCLUSIONS

The two types of speed control explored in this work are the dynamic and static methods. In the dynamic method power is handled by rotating machinery twice. The static method involves controlling the applied frequency, and or, voltage to either an induction motor or a d-c motor.

There are many advantages for chosing an a-c motor over a d-c motor. Some of these are:

1. Lower maintenance due to the absence of carbon brushes and commutator.
2. Lower weight per horsepower.
3. Higher speed range.
4. Higher efficiency over a wider operating speed.
5. Operating ability in an explosive environment.

The advent of the silicon-controlled rectifier and the rapid increase in its power handling capacity has made it feasible to build static inverters at drastically reduced cost. Such systems are compact, reliable and efficient.

The ability to use the versatile characteristics of the semiconductor inverter to achieve optimized control of an induction motor presents many design alternatives. The most common control technique is constant volts/hertz operation. This method results in constant torque up to the motor frequency rating and constant power above the rated frequency.

Slip control through frequency feedback is insurance that the motor will always operate at high efficiency and power factor.

The solid state inverter has been found useful in a variety of situations. Among these are railroad rolling stock, conveyor speed regulations and electric vehicle propulsion. In an electric vehicle the static inverter and electric motor replace the standard gasoline motor, transmission and drive shaft. Great improvements in the field of energy storage capacity will have to be achieved before the electric system can be practical.

The harmonic content of the voltage waveform from the inverter presents the motor with energy which must be dissapated as heat. Dependent on power source harmonic content and motor load, motor sizing may become critical because of thermal limitations. Experimental work has proven the fundamental frequency to be the only contributor of useful energy. Various mentods of harmonic reduction have been suggested. Two such methods are:

1. Waveform harmonic reduction through control of power device conduction time.
2. Series and parallel filters for reduction of harmonic content before power arrives at motor terminals.

The effects these harmonic reduction techniques have on the overall performance of the system would have to be evaluated. The encouraging correlation between test and calculated data confirm the idea that harmonic superposition techniques are applicable to this type of motor analysis.

BIBLIOGRAPHY

BIBLIOGRAPHY

Agarwal, P. D. The GM High Performance Induction Motor Drive Systems. New York: IEEE Trans. Paper No. 68TP 107-PWR, 1969.

Campbell, S. J. Static Power Supplies With A-C Machines. Pittsburg, Pennsylvania: Westinghouse Engineer, Volume 32, No. 2, 1972.

Cheng, David K. Analysis of Linear Systems. Reading, Massachusette: Addison-Wesley Publishing Company, Inc., 1961.

Del Toro, Vincent. Electromechanical Devices for Energy Conversion and Control Systems. Englewood Cliffs, New Jersey: Prentice-Hall, Inc., 1968.

Fulks, Watson. Advanced Calculus. New York: John Wiley and Sons, Inc., 1969.

Johnston, Richard W. Modulating Inverter System for Variable Speed Induction Motor Drive (GM Electrovair II). New York: IEEE Trans. Paper No. 68TP 108-PWR, 1967.

Klingshirn, Eugene A., and Howard E. Jordan. Polyphase Induction Motor Performance and Losses on Nonsinusoidal Voltage Sources. New York: IEEE Trans Paper No. 31TP 67-472, 1967.

Pelley, B. R. Thyristor Phase Controlled Converters and Cycloconverters. New York: Wiley Interscience, 1971.

Reed, Henry R. Electrical Engineering Experiments. New York: John Wiley and Sons, Inc., 1948.

Salihi, Jalal T. Induction Motor Control Scheme for Battery Powered Electric Car (GM Electrovair I). New York: IEEE Trans. Paper No. 68TP 22-IGA, 1968.

Speckhart, Frank H., and Walter L. Green. A Guide to Using CSMP. Englewood Cliffs, New Jersey: Prentice-Hall, Inc., 1976.

Test Procedure for Polyphase Induction Motors and Generators. New York: IEEE Standards, 1964.

Wakefield, Earnest H. An A-C Drive Electric Vehicle. New York: IEEE Trans. Paper No. TOD-73-87, 1973.

APPENDIXES

APPENDIX A

COMPUTER PROGRAMS

Three computer programs were used in this work, and the common language was the Continuous System Modeling Program (CSMP).[10] The objective was to have the computer perform the repetitive work involved in processing and comparing experimental data. CSMP greatly extends and simplifies computer solution of real world problems. A very brief discussion of the programs follows.

Program I solves the motor equivalent circuit. The multiple data run feature of CSMP is used to make six consecutive data runs for different values of slip. The calculations are all simple algebraic manipulations, and twelve calculated parameters are printed out for each data run.

Program II calculates the Fourier Coefficients for a given waveform. The waveform in question is broken down into K discrete steps and values for each of these K steps is entered into the program as a data point in a vector. The program calculates the harmonic content for each of these K steps and prints the results. Dividing the waveform into smaller steps will increase the accuracy.

Program III was used to synthesize the current waveshape

---

[10] Frank H. Speckhart, A Guide to Using CSMP--The Continuous System Modeling Program (Englewood Cliffs: Prentice-Hall, Inc., 1967).

flowing through the motor. Each harmonic has its phase, amplitude and frequency entered into the computer as a data point. The harmonics were combined; the composite waveform, XTOT, was plotted and this plot was then used for comparative purposes.

PROGRAM I. COMPUTER SOLUTION OF EQUIVALENT CIRCUIT

```
Initial
     PARAM R1=4.95,R2=2.27,RM=637.0,WRW=100
     PARAM X1=5.16,X2=5.16,E1=107.4,WC=46.,XM=82.2
     PARAM S=(.01,.02,.025,.03,.04,.05)
     GM=1.0/RM
     BM=1.0/XM
     X2=X1
NOSORT
     Z2=SQRT((R2/S)**2.0+(X2)**2.0)
     G=(R2/(S*Z2**2.0))+GM
     B=(X2/(Z2**2.0))+BM
     Y=SQRT(G**2.0+B**2.0)
     R=G/(Y**2.0)
     RO=R+R1
     X=B/(Y**2.0)
     XO=X1+X
     ZO=SQRT(RO**2.0+XO**2.0)
     PF=RO/ZO
     A1=E1/ZO
```

```
      WI=3.0*(A1**2.0)*R0
      WS=3.0*(A1**2.0)*R1
      WR=S*(WI-WS)
      WRW1=(1.0-S)*WRW
      LOSS=WS+WR+WC+WRW1
      P0=WI-LOSS
      EFF=(1.0-(LOSS/WI))*100
      WRITE(6,100)Z2,R0,X0,Z0,PF,A1,WI,WS,WR,LOSS,P0,EFF
100   FORMAT(1H ,10X,F12.4)
101   FORMAT(1H ,5X,12HNEW DATA RUN)
```

PROGRAM II. COMPUTER EVALUATION OF FOURIER COEFFICIENTS

```
Initial
      Storage V(750)
      K=360
      K0=K-1.0
      Z=6.2832
      I=1.0
      N=1.0
      Table V(1=36)=36*(.5),V(37-120)=84*(1.),V(121-156)=36*(.5)
      Table V(157-180)=24*(0.0),V(181-216)=36*(-.5),
      Table V(217-300)=84*(-1.),V(301-336)=36*(-.5),
      Table V(337-360)=24*(0.0)
      K1=1.0/K0
NOSORT
      WRITE(6,100)
```

```
      DO 1 N=1,20
      AO=0.0
      AN=0.0
      BN=0.0
      DO 2 I=1,360
      AO=AO+V(I)*K1
      A=N*K1*(I-1.0)
      Z1=A*Z
      AN=AN+V(I)*K1*COS(Z1)
      BN=BN+V(I)*K1*SIN(Z1)
    2 CONTINUE
      AN=AN*2.0
      BN=BN*2.0
      WRITE(6,101)N,AN,BN
    1 CONTINUE
      WRITE(6,102)AO
  102 FORMAT(/1H,3HAO=,4X,F6.2)
  101 FORMAT(H,I4,2F12.4)
  100 FORMAT(/1H,2X,1HN,7X,2HAN,7X,2HBN
```

PROGRAM III. COMPUTER SYNTHESIS OF CURRENT WAVEFORM

```
      PARAM P1=.8,V1=3.0
      PARAM F1=125.6,F3=377.,F5=628.,F7=879.6,F9=1131.
      PARAM F11=1382.3,V3=1.66,V5=.645,V7=.340,V9=.210,V11=.14
      PARAM P3=1.06,P5=1.2,P7=1.32,P9=1.36,P11=1.4
      X1=V1*SINE(0.0,F1,P1)
```

```
X3=V3*SINE(0.0,F3,P3)
X5=V5*SINE(0.0,F3,P3)
X7=V7*SINE(0.0,F7,P7)
X9=V9*SINE(0.0,F9,P9)
X11=V11*SINE(0.0,F11,P11)
XTOT=V1+V3+V5+V7+V9+V11
PRTPLT XTOT
TIMER FINTIM=.1,OUTDEL=0.00195
```

APPENDIX B

TEST EQUIPMENT

The following is a listing of test equipment used to accumulate the experimental data for this work.

Motor Torque:

The a-c motor was loaded with a d-c motor, General Electric 1 and 1/2 hp, 115 volts. The d-c motor's mounting plates were bearing mounted so the motor could rotate freely. Attached to the d-c motor was a strain gauge, Chatillon 25 lbs., preloaded with a 10 lb. weight. The movement arm between the scale and motor was 5 and 1/4 inches. Each of the two motors had a 1 inch diameter shaft, and they were connected with a Lovejoy coupling and spider. The d-c motor was excited from a 0 to 200 volt d-c source, the field load was adjustable from 2 to 12 ohms.

Motor Speed:

A strobe, General Radio Strobotac type 1531 connected to an electronic counter, Hewlett Packard model number 5303 A, measured motor rpm. The strobe was set at twice motor speed to reduce error.

Resistance:

Leeds and Northrup Company Galvanometer Test Set Number 5300.

Current:

Weston Model Number 433.

Voltage:

General Electric A-C Voltmeter Scales 150, 300, 600.

Power:

Single phase--Weston Power Meter.

Three phase--Weston Model Number 329.

Waveforms:

Voltage waveforms were taken using a storage scope Hewlett Packard Model Number 181 A with 1807 A vertical amplifier and 1820 C time base. Current waveforms were taken using the same scope with a Tektronix P5021 a-c current probe and Type 134 current probe amplifier.

Figures 39, 40 and 41 are photographs taken of the laboratory equipment and test fixtures.

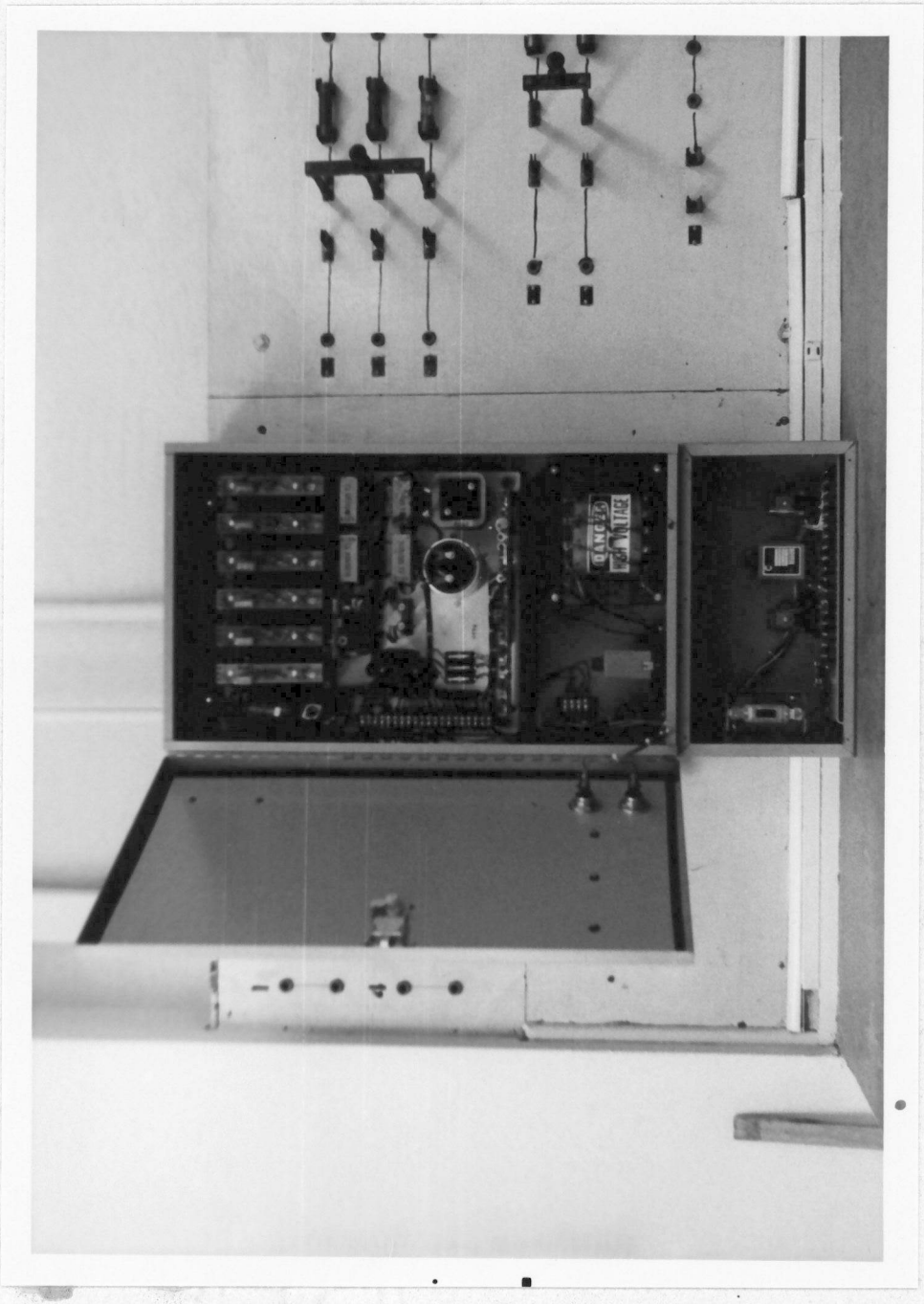

Figure 39. Solid State Inverter

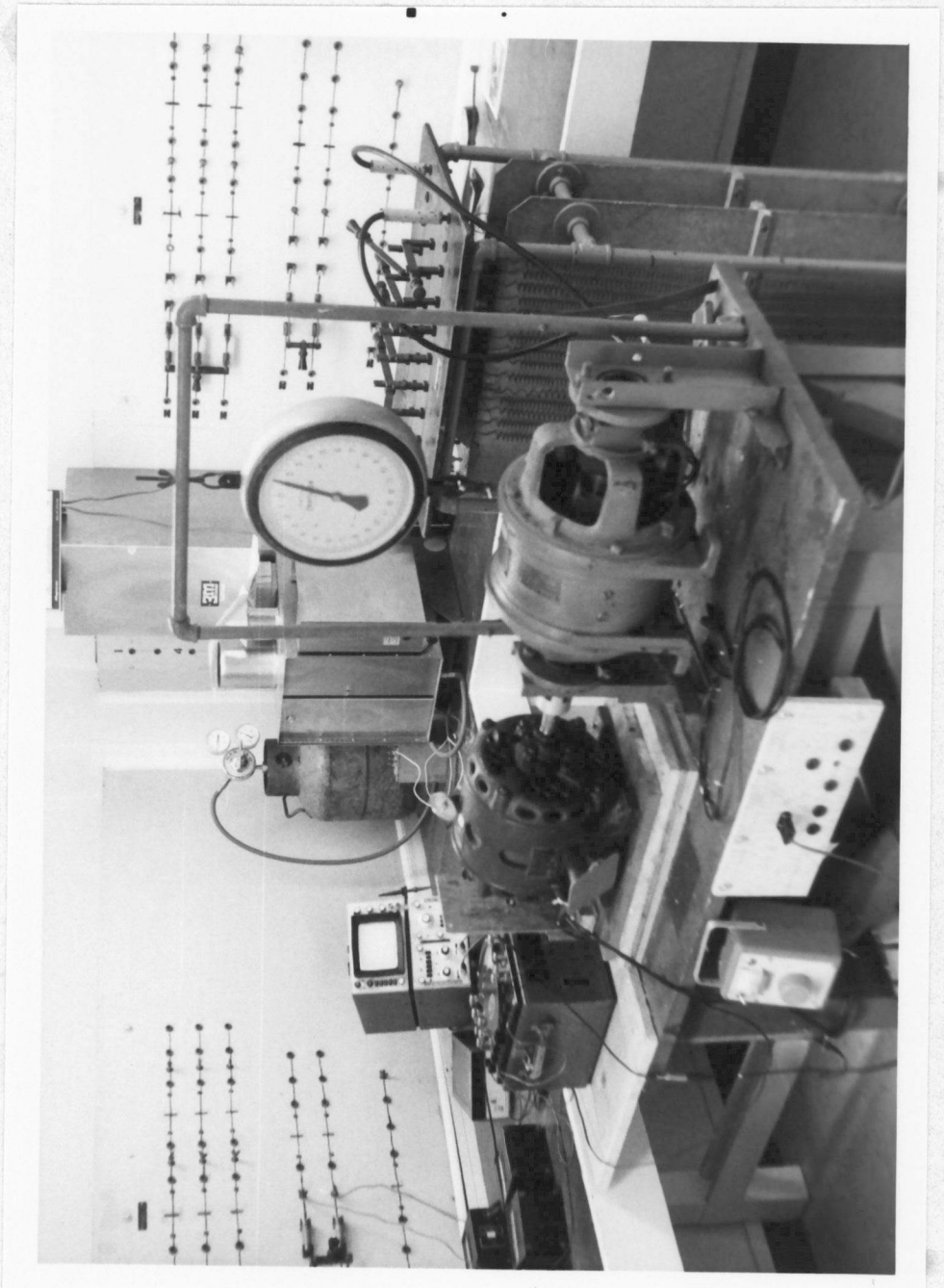

Figure 40. A-C Test Motor and D-C Load Motor

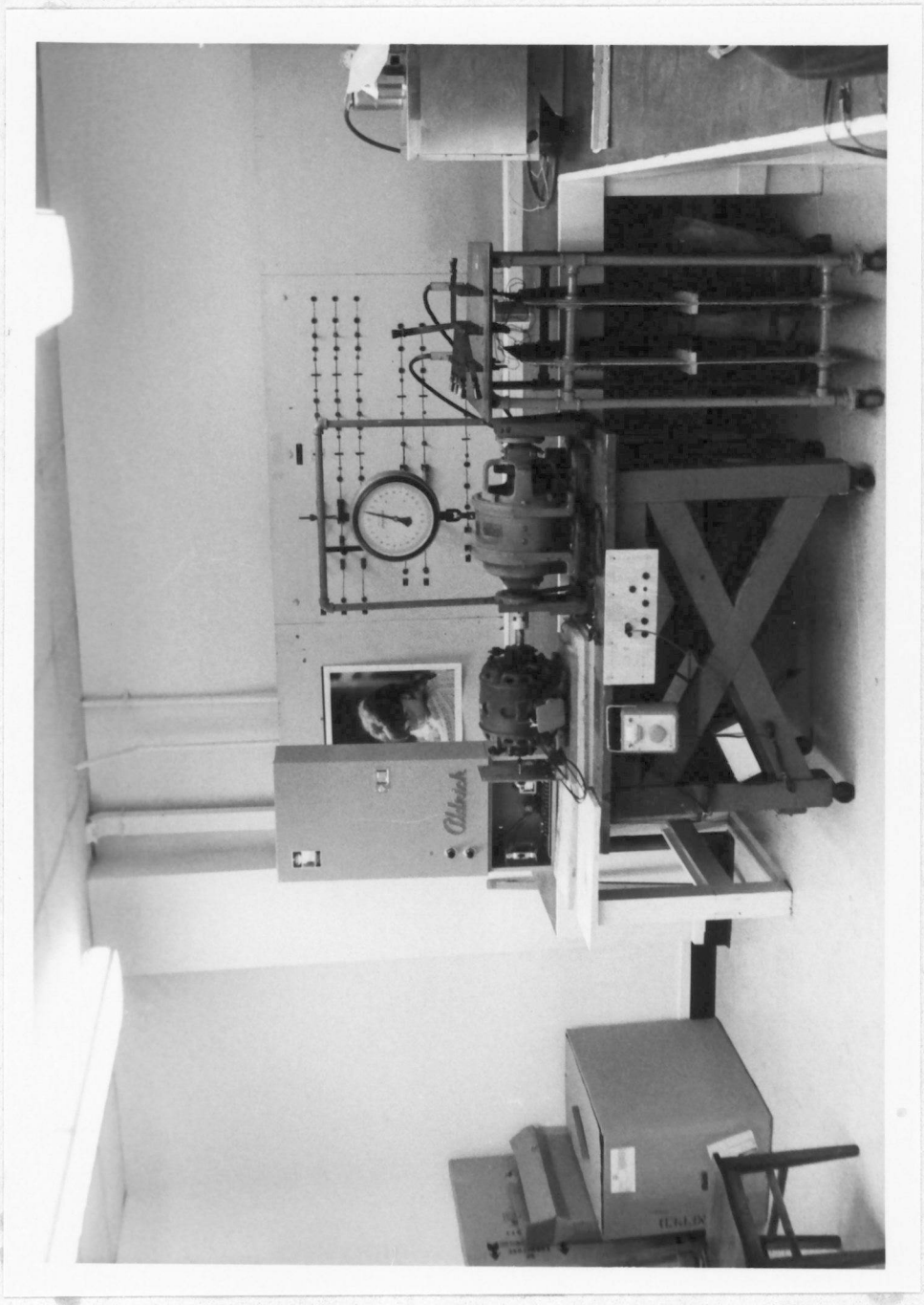

Figure 41. Complete Test Station

VITA

Clement C. Morlock Jr. was born in Indianapolis, Indiana on April 9, 1948. He has since lived in Michigan City, Indiana, Hollywood, Florida and Greeneville, Tennessee. Clement graduated from Greeneville High School in 1965 and attended Christian Brothers College in Memphis, Tennessee. After two years of pre-engineering at Christian Brothers College he attended the University of Tennessee in the Electrical Engineering department. In the spring of 1971 he received a Bachlor of Science in Electrical Engineering.

Following graduation Clement accepted a job with the Magnavox Company of Fort Wayne, Indiana. He has been located at the Greeneville and Jefferson City, Tennessee manufacturing facilities. While working for the Engineering department he has attended graduate school at the University of Tennessee. The author is married to the former Miss Cynthia Erickson of Harrisonburg, Virginia.